



**British
Geological Survey**
NATIONAL ENVIRONMENT RESEARCH COUNCIL

Challenge 1 (Hazards) Final Report



Challenge 1 (Hazards) Final Report

S. Loughlin, M. Pagani, V. Poggi, P. Henshaw, F. Løvholt, B. kalsnes, C. Christenson, S. Jenkins, H. de Moel, T. Veldkamp, T. Stolte, F. Nadim, R. Rudari, L. Rossi, M. Nayembil

Contributors

G. Mbogoni, M. Msechu, G. Kamihanda, A. Masanja, A. Bushi, M. Msabi, P. Sangana, W. Kikwasi, H. Mtongori, J. Kijazi

Contents

Contents.....	iii
Summary	8
1 Introduction	9
1.1 Challenge 1: Multi-hazard Data Schema and Database	9
1.2 Outline of the report	10
2 Data standards and data schema	11
2.1 Introduction	11
2.2 GFDRR-DfID Challenge Fund Expert Workshop in London.....	11
2.3 Data standards for the challenge fund scenarios	13
2.4 Data schema.....	13
2.5 “Event Set” entity	15
2.6 “Event” entity	16
2.1 “Footprint SET” entity.....	17
2.2 “Footprint” entity.....	18
2.3 Uncertainty	19
2.4 Data schema compilation example	20
2.5 Populating the database	22
3 Earthquake hazard scenarios.....	23
3.1 Introduction	23
3.2 PSHA results in Tanzania.....	23
3.3 Disaggregation.....	26
3.1 Fault scenario definition	30
3.2 Ground motion field simulation	31
4 Volcanic ash fall hazard scenarios.....	32
4.1 Introduction	32
4.2 Chosen volcano.....	32
4.3 Eruption scenarios	33
4.4 Method, metadata and results	35
4.5 Summary.....	40
5 Landslide hazard scenarios	41
5.1 Introduction	41
5.2 Scenario methodology	41
5.3 Summary.....	46
6 Tsunami hazard scenarios	49
6.1 Introduction	49

6.2	Tsunami hazard methodology and results	49
6.3	Summary.....	56
7	Flooding hazard scenarios.....	58
7.1	Introduction	58
7.2	Methodology.....	58
7.3	Results	59
8	Drought hazard scenarios.....	61
8.1	Historical droughts	61
8.2	Indicators	63
8.3	Comparison.....	65
9	Overall guidance and use considerations.....	67
10	References	68
11	Appendix 1 scenario examples	70
11.1	Landslide Event Data	70
11.2	Flood event data	71

FIGURES

Figure 1 Entity-relationship diagram of the proposed data-model	14
Figure 2 Probabilistic seismic hazard map computed for Tanzania using the model developed by Poggi et al. (2017). In this example, calculation is done for 475 years return period at PGA (top) and spectral acceleration at 0.2 seconds (bottom).	24
Figure 3 Hazard curves computed for the town of Dodoma (Tanzania) using the model developed by Poggi et al. (2017). In this example, calculation is done for 50 years investigation time at PGA (top) and spectral acceleration at 0.2 seconds (bottom). The value at 10% probability of exceedance is printed in each panel.....	25
Figure 4 Uniform Hazard Spectrum (UHS) computed for the town of Dodoma (Tanzania) using the model developed by Poggi et al. (2017). In this example, calculation is done for 10% probability of exceedance in 50 years.	26
Figure 5 Mean disaggregation Magnitude-Distance-Epsilon computed for PGA with 10% probability of exceedance in 50 years (top) and spectral acceleration at 1 second with 10% probability of exceedance in 50 years (bottom).	27
Figure 6 Mean geographical (Latitude-Longitude) disaggregation computed for spectral acceleration at 1 second with 10% probability of exceedance in 50 year, showing the contribution of different magnitudes; in the bottom panel we present the case for magnitude 7.75, which shows a particularly pronounced directionality (less pronounced at lower magnitudes).	28
Figure 7 Orientation of the 7 faults assumed compatible with the hazard scenario from disaggregation of the Dodoma region. We plot in the background the fault dataset of Macgregor 2015 (thin red lines) and the area source zones included in model of Poggi et al. 2017.	29

Figure 8 Rupture trace length as a function of magnitude computed using the Wells and Coppersmith (1994) scaling relation and three different aspect ratios.....	29
Figure 9 Example of ground motion field computed in the area of Dodoma for different the faults. Although the simulated magnitude scenario is identical between realizations (M 6), the absolute value of the ground motion is noticeably different due to the different sampling of the GMPEs uncertainty.	30
Figure 10 Holocene volcanoes within Tanzania (taken from the Global Volcanism Program www.volcano.si.edu), with the capital cities and study volcano highlighted (modified from Brown et al., 2015).	33
Figure 11 Frequency-magnitude relationship for Rungwe, which acted as an analogue for Fentale, Longonot and Suswa volcanoes, derived through expert elicitation. The solid line represents the mean estimate and the dashed lines the interquartile confidence bounds.	34
Figure 12 Wind direction (left) and speed (right) averaged by month, with height above surface, for the ECMWF ERA-Interim 6 hourly reanalysis data used in this study (2005-2014).....	36
Figure 13 The hazard footprint for a VEI 2 explosive eruption scenario at Rungwe volcano.....	38
Figure 14 The hazard footprint for a VEI 4 explosive eruption scenario at Rungwe volcano.....	39
Figure 15 The hazard footprint for a VEI 6 explosive eruption scenario at Rungwe volcano.....	39
Figure 16 Tanzania landslide susceptibility map (Kilimanjaro region with high susceptibility marked in red).....	43
Figure 17 Landslide susceptibility north of Moshi.	44
Figure 18 Watersheds northeast of Moshi.	45
Figure 19 Figure by Rickenmann (2005) showing relationships between the ratio of decrease in elevation to runout distance ($\tan \beta$) and the volume of mass movement. The dashed line shows the approximate boundary that bounds the Swiss debris flow events compiled by Corominas (1996).	46
Figure 20 Sketch of landslide affected zones north Moshi, Kilimanjaro region.....	47
Figure 21: Sketch of landslide affected zones east of Moshi, Kilimanjaro region.....	48
Figure 22 Sumatra-Andaman Trench scenarios, maximum surface elevation. Upper Mw8.6 scenario, lower Mw9.3 scenario.	51
Figure 23 Coastal inundation heights for Sumatra-Andaman Trench scenarios. Upper panels M _w 8.6 scenario, lower panels M _w 9.3 scenario. Left panels, mean values. Right panels, 90 percentile inundation heights.....	52
Figure 24 Sumatra Trench scenarios, maximum surface elevation. Upper M _w 8.8 scenario, lower M _w 9.5 scenario.	53
Figure 25 Coastal inundation heights for the Sumatra Trench scenarios. Upper panels M _w 8.8 scenario, lower panels M _w 9.5 scenario. Left panels, mean values. Right panels, 90 percentile inundation heights.....	54
Figure 26 Makran Trench scenarios, maximum surface elevation. Left M _w 8.7 scenario, right M _w 9.3 scenario.	55
Figure 27 Coastal inundation heights for the Sumatra Trench scenarios. Upper panels M _w 8.8 scenario, lower panels M _w 9.5 scenario. Left panels, mean values. Right panels, 90 percentile inundation heights.....	56
Figure 28 The conceptual modelling framework used for flood hazard scenarios.	58

Figure 29 Schematic showing full computation of the scenarios.....	59
Figure 30 a. One of the largest simulated events in the coastal zone of Tanzania. b. One of the largest simulated events country-wide in Tanzania. c. One of the largest simulated events in southern Tanzania.....	60
Figure 31 Comparison of drought events according to three databases, including their spatial extent according to the sources.....	62
Figure 32 SPEI (left) and SSFI (right) for various return periods (denoted by X).	64
Figure 33 Water crowding index. Values below 500 m ³ /capita/year indicate extreme water scarcity.....	64
Figure 34 Comparison of drought indicators for the 1984 drought event in Tanzania. Drought intensity is the accumulated deficit (using a threshold of -1).....	65

TABLES

Table 1. Consortium institutions and perils/hazards.	10
Table 2 Common hazards and hazard intensities with characteristics that could be captured/considered as they affect impact.....	12
Table 3 The hazards and hazard intensities for which test scenarios were developed in the Challenge Fund 1 project.....	13
Table 4 ‘Event set’ entity attributes	15
Table 5 ‘Event’ entity attributes.....	16
Table 6 ‘Footprint entity’ attributes	17
Table 7 The proportion of the explosively erupted material that is dispersed in the atmosphere as tephra (as opposed to collapsing as pyroclastic density currents).	37
Table 8 The height of the erupting column above the volcanic vent for each scenario.....	37
Table 9 Estimated debris flow volumes	43
Table 10 Earthquake scenario fault parameters	49

Summary

This final report provides a summary of the activities and contributions to the ‘Hazard’ consortium of the GFDRR/DfID Challenge Fund (2nd round) since April 2017. Using Tanzania as a pilot study, we developed a multi-hazard data schema and prototype database based on seven perils and associated hazards: droughts, earthquakes, floods, landslides (earthquake and rainfall induced), storm surges, tsunamis and volcanoes. We are discovering synergies and common ground between different hazards and perils enabling a robust data schema to be developed. The data schema and prototype database is scalable globally and has been tested with data from neighbouring countries in the region (Ethiopia, Malawi, Kenya, Uganda and Mozambique).

We worked closely with the Exposure and Vulnerability Challenge groups in order to provide relevant data on hazard intensities, known vulnerability analyses and exposure taxonomies, building synergies across the consortia.

The consortium also engaged with global partnerships for different hazards (e.g. GEM, GVM), gathering feedback from other stakeholders (e.g. reinsurance sector at the July 2017 workshop) and Tanzanian partners (e.g. Geological Survey of Tanzania), and the international research community. We followed the Sendai Framework for Disaster Risk Reduction (SFDRR) which recommends that science and technology should be coordinated through existing networks and scientific research institutions at all levels and in all regions (UNISDR, 2015).

This report summarises the final project outcomes, gives some guidance on use of the outcomes and recommendations for next steps.

1 Introduction

The ‘Challenge Fund’ is an initiative of the Global Facility for Disaster Reduction and Recovery (GFDRR) and the UK Department for International Development (DfID) supporting activities that will promote the creation and use of risk-related data. The Challenge Fund second round focuses on the intention to expand the effort to reduce disaster risk management costs and increase resilience by developing a framework that facilitates a multi-hazard view of risk. This new multi-hazard risk framework will be applied in predominantly data-poor regions where traditionally the lack of data has proven a barrier to the application of risk models. Three Challenges worked closely together:

Challenge 1: Develop a Data Schema and Data for a Multi-hazard Database. This consortium is led by the British Geological Survey (BGS).

Challenge 2: Develop a Data Schema and Data for a Global Exposure Database. This consortium is led by the Global Earthquake Model (GEM).

Challenge 3: Develop a Data Schema for a Global Database of Vulnerability Functions. This consortium is led by the UCL EPICentre.

All three data schemas are interoperable and adopt the same taxonomy. The data schema and risk framework has been demonstrated for Tanzania and can be scaled up for application in any other country.

1.1 CHALLENGE 1: MULTI-HAZARD DATA SCHEMA AND DATABASE

The main goal of the Challenge Fund project was to design a data schema for multiple hazards with defined data standards and develop a prototype hazards database populated by some test scenarios. In order to achieve these objectives, the consortium brought together expertise from at least five disciplines: geology, geophysics, meteorology, oceanography and informatics.

Challenge 1 is a consortium of ten institutions (with associated networks), three of whom are based in Tanzania (Table 1) who addressed seven hazards: droughts, earthquakes, floods, landslides, storm surges, tsunamis and volcanic eruptions. We also investigated interacting hazards, for example earthquake-triggered landslides and tsunamis, and landslides triggered by intense rainfall.

These hazards and interacting hazards all require different approaches and are all at different stages in terms of global data availability, access to models, and progress towards risk assessments. Nevertheless, we consider this a useful challenge to investigate synergies, common approaches and to identify knowledge gaps and barriers to progress.

We define the term ‘multi-hazard’ as multiple hazards (more than one) and the potential interactions between hazards, following the revised UNISDR definition of multi-hazard (UNISDR, 2017):

- (1) selection of multiple major hazards that the country faces, and (2) specific contexts where hazardous events may occur simultaneously, in a cascading fashion or cumulatively over time, and taking into account the potential interrelated effects.

The objectives of the Challenge 1 project were:

- the construction of a data schema to handle multiple hazards and their corresponding perils,
- the calculation of a number of scenarios for different perils (compatible with the vulnerability functions that will be defined within Challenge 3),
- to develop guidance on database maintenance, hosting, access and use,
- to provide evidence on how the approach can be scaled globally, and
- to provide in-country training.

In meeting these objectives, Challenge 1 delivered six project outputs:

- an inception report
- a set of standards for delivery of hazard data;
- an extensible database schema;
- a prototype hazards database;
- a technical report including guidance on database maintenance, access and hosting.
- Delivery and guidance at a final workshop.

Table 1. Consortium institutions and perils/hazards.

Institution	Perils/hazards
British Geological Survey (BGS)	Multi-hazard, Volcano (ash fall)
Global Earthquake Model (GEM)	Earthquake
Earth Observatory of Singapore (EOS)	Volcano (ash fall)
Norwegian Geotechnical Institute (NGI)	Landslide (earthquake and rainfall-triggered), Tsunami (earthquake-triggered)
National Oceanographic Centre (NOC)	Storm surge
Centro Internazionale in Monitoraggio Ambientale (CIMA Foundation)	Flood
Institute for Environmental Studies at the University of Amsterdam (IVM)	Drought
Geological Survey of Tanzania (GST)	Earthquakes, volcanic eruptions, landslides
Tanzanian Meteorological Agency (TMA)	Floods, tsunami, storm surge
University of Dodoma (UD)	Earthquake, flooding, landslide

1.2 OUTLINE OF THE REPORT

After the introduction (Chapter 1), this report describes the data schema, data standards and database in Chapter 2, scenarios and particular issues related to each hazard are listed in chapters 3-7, guidelines on the use of the proto-database are provided in Chapter 8 and final conclusions are presented in Chapter 9. Annexes contain some of the scenarios.

2 Data standards and data schema

2.1 INTRODUCTION

This project was tasked to design an *extensible* data schema so we have considered a wide variety of hazards that cover a broad range of hazard types, hazard intensity measures and approaches to hazard assessment. For example, for earthquakes probabilistic seismic hazard assessment is well-established whereas for drought, indices are used.

In addition to consultations within our own consortium and networks, a consultation event was held with stakeholders in insurance and reinsurance in London where hazard intensity measures were discussed to establish which were the most important for users.

As a result of discussions in London, several additional hazards were considered during development of the data schema even though they weren't tested with scenarios during the project.

2.2 GFDRR-DFID CHALLENGE FUND EXPERT WORKSHOP IN LONDON

This expert workshop took place at XL Catlin in London on July 27th 2017 and was led the Challenge Fund leads: UCL EPICentre, British Geological Survey and Global Earthquake Model Foundation. The purpose of the workshop was to gather stakeholders together into a consultation process to help bridge the gap between theoretical formulations of hazard, exposure and vulnerability and practical applications. Participants included representatives from the insurance and reinsurance London market, academic institutions, engineering companies, risk modelling companies, NGOs, GFDRR and DfID representatives.

The objective of the workshop was to gather information contributing to the development and validation of three data schemas for the representation of hazard, exposure and vulnerability data in a developing country context. Feedback was gathered based on roundtable discussions using well-known participatory research approaches. Key topics discussed included:

1. Single, multiple and multi-hazard characteristics
2. Physical vulnerability characteristics and exposure taxonomy
3. Social vulnerability characteristics and indicators
4. Scoring vulnerability indicators and datasets
5. Data schema uses and challenges in scaling globally

A workshop report has been produced which provides full details of the event and its context.

2.2.1 Hazards and hazard intensities

The data schema must be extensible and applicable in many developing countries so must consider hazards beyond those represented by the expertise in the Challenge 1 consortium.

Common and useful hazard intensities that are used in hazard assessment and were mentioned during the London workshop are listed in Table 2. There was additional discussion about the characteristics of the particular hazard that could also be captured (*italics*) as they strongly affect impact. These discussions and the various different hazards and approaches to hazard assessment were considered during the design of the data schema.

Table 2 Common hazards and hazard intensities with characteristics that could be captured/considered as they affect impact.

Primary hazard	Hazard process	Hazard intensity measure	Characteristics
Flood		water depth	velocity, duration, debris content
Tsunami		water depth	velocity, run-up (horizontal extent), debris content
Storm surge		water depth	velocity, run-up (horizontal extent), debris content, types of wave
Volcanic eruption	Ash fall	ash fall thickness	wet or dry, duration,
Volcanic eruption		ash fall loading	
Volcanic eruption	Pyroclastic density current	inundated area	currently considered binary
Volcanic eruption	Lava flow	inundated area	currently considered binary
Volcanic eruption	Lahars	inundated area	currently considered binary
Volcanic eruption	Lahars	water depth (m)	velocity, duration, debris content
Earthquake	ground shaking	(PGA, PGV, spectral acceleration)	duration, EMS, MMI
Earthquake	seismic intensity		capturing historical descriptions and evidence
Earthquake	liquefaction	permanent ground deformation (PGD)	
Earthquake	ground failure	permanent ground deformation (PGD)	
Landslide		inundated area	can be considered binary
Landslide		permanent ground deformation (PGD)	maximum force, debris content
Cyclone		peak (or average) wind speed, central pressure	category of storm, duration
Drought	precipitation and temperature	Standardised precipitation evapotranspiration index (SPEI)	
Drought	(many types and indices ¹)		
Tornado		peak (or average) wind speed, central pressure.	
Severe convective storm		peak wind speed	altitude
Precipitation		rate	
Hail		size	Kinetic energy
Lightning		frequency	
Extreme heat		temperature	humidity
Fire		Burnt area	duration

¹ World Meteorological Organization (WMO) and Global Water Partnership (GWP), 2016: *Handbook of Drought Indicators and Indices* (M. Svoboda and B.A. Fuchs). Integrated Drought Management Programme (IDMP), Integrated Drought Management Tools and Guidelines Series 2. Geneva.

2.3 DATA STANDARDS FOR THE CHALLENGE FUND SCENARIOS

In general, the hazards considered in this project have all been modelled previously at a global scale (e.g. for GAR15). Nevertheless, data availability is highly variable across the hazards. For some hazards, there are global datasets available from which scenarios can be derived at a national scale (e.g. earthquakes) however for some other hazards, the primary data simply has not been collected for large parts of the developing world (e.g. volcanic eruption) and national scale hazard assessments are not always appropriate. For volcano and tsunami, significant knowledge gaps must be accommodated using techniques such as expert elicitation. In this project, existing data (e.g. from GAR15 and previous GFDRR studies) have been used to generate hazard scenarios which have a range of characteristics (e.g. likelihood, return periods etc).

For the chosen hazards (Table 3), good practice in hazard assessment has been followed, using methods supported by peer-reviewed publications and these different methods were the primary drivers in designing and testing the data schema. In addition to the main hazards listed, we considered how interacting (cascading) hazards could be represented in a data schema.

Table 3 The hazards and hazard intensities for which test scenarios were developed in the Challenge Fund 1 project.

Hazard	Process	Hazard intensity
Earthquake	Ground shaking	Peak Ground Acceleration
Volcanic eruption	Ash fall	Ash fall loading
Flood	Flood	Water depth
Tsunami	Tsunami	Inundated area
Landslide	Landslide	Inundated area
Drought	Drought (precipitation and temperature)	SPEI

2.4 DATA SCHEMA

2.4.1 Database terminology

Data schema – the organisation of data as a blueprint of how a database is constructed.

Hierarchical database – Uses a tree structure to link a number of disparate elements to one ‘parent’ primary record.

Entity – any object in the system that we want to model and store information about. It can be classified and have stated relationships to other entities. The attributes of entities are stored as records.

Attribute – is a characteristic of an entity object.

Relationships – Relationships allow relational databases to split and store data in different tables, while linking disparate data items.

Entity-relationship diagram – A graphical representation of entities and their relationships to each other.

2.4.2 Data structure

The proposed data structure is meant to store hazard scenarios (footprints) and the associated information that describes those scenarios and how they were modelled (sometimes referred as meta-data or meta-information). The data structure contains three main entities hierarchically organised as follows (from the top to the bottom):

- The “Event set”
- The “Event“
- The “FootprintSet”
- The “Footprint”

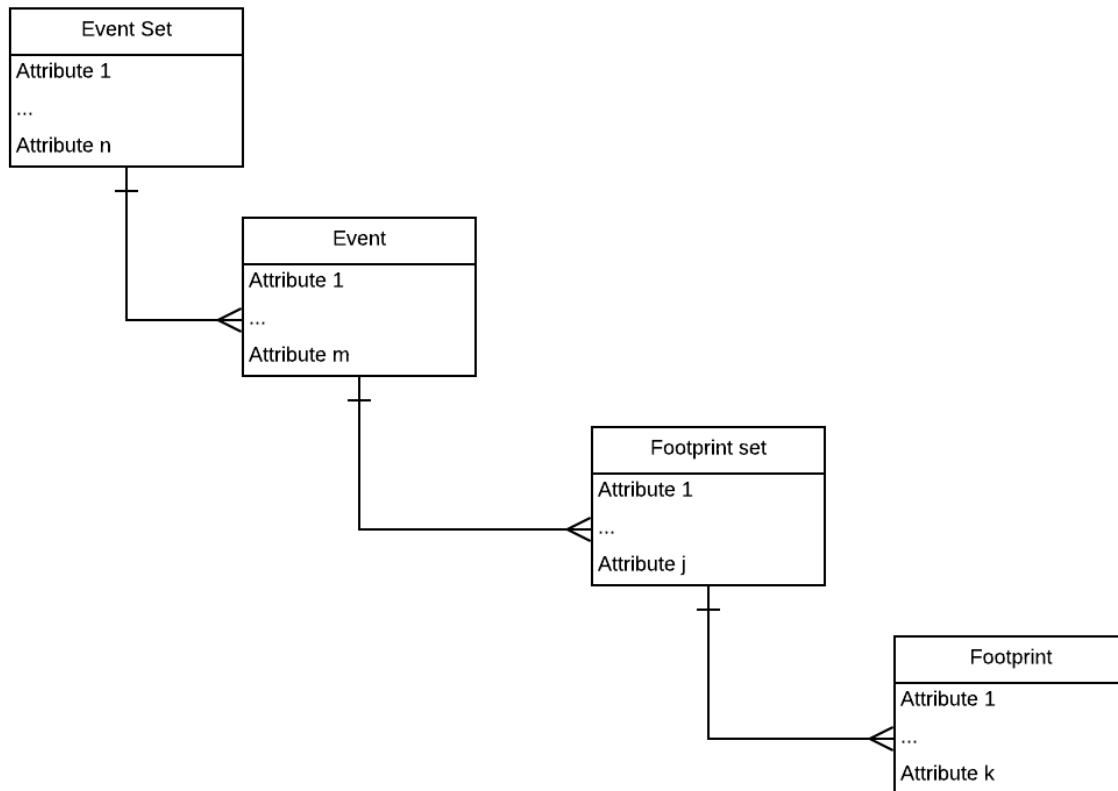


Figure 1 Entity-relationship diagram of the proposed data-model

In an entity-relationship data-model, the relationship between the four entities is a *one-to-many* relationship (from top to bottom). The “Event set” is the most comprehensive container of information, designed to store scenario data for a specific analysis such as an earthquake scenario analysis for a nation or a city or a volcano ash-fall hazard analysis. One ”Event set” entity is associated to many “Event” entities since for a scenario analysis it is common to define a finite set of events normally representing either the most adverse cases (e.g. ‘reasonable worst case’ scenario) or the most representative occurrences (e.g. ‘most likely’ scenario) for a given return period (or set of return periods). For example, in the case of an earthquake scenario risk analysis it is common to select some earthquakes representing the most severe earthquakes generated by the faults surrounding the investigated site. Each modelled earthquake would be represented by an Event of a Event set.

The lowermost entities in this hierarchical structure are the “Footprint set” and “Footprint”. The footprint is one possible realisation of an event. The “Footprint Set” is a container for one or several “Footprints” representing the same intensity measure type. In this case the one-to-many association accommodates cases where an “Event” is represented by a number of realisations (i.e. many “Footprint”s) accounting for the uncertainty associated with a specific event. Note that the uncertainty of a “Footprint” can be alternatively described by the second moment of a probabilistic distribution or by a discrete distribution (i.e. discrete histogram at each point illustrating the probability of occurrence of a discrete set of values of a specific intensity measure type). Both descriptions of uncertainty can be fixed (i.e. constant over the spatial extent covered by the corresponding footprint) or spatially variable. For example, for an earthquake hazard scenario analysis, it is customary to simulate many scenarios for a single “Event” to account for the uncertainty in the calculation of the spatial distribution of shaking for a given intensity measure. Using the proposed data schema all the scenarios referring to a specific event computed for a given intensity measure type are grouped into a “Footprint set”.

2.5 “EVENT SET” ENTITY

The “event set” entity contains information on the events considered for a given area. Every “event set” instance will have the following attributes (the green background shows the attributes considered mandatory in order to create a footprint). The description and bibliography are critical as this is where the model used, data sources, assumptions, references, acknowledgements, purpose and IPR of an event set is described.

Table 4 ‘Event set’ entity attributes

Parameter	Description
id	A unique identifier [str]
geographic_area_bb	A bounding box i.e a (minimum latitude, minimum longitude, maximum latitude, maximum longitude) tuple. It is used to outline the investigated area. Can be used for a quick preliminary retrieval of information given an area. [float, float, float, float] - Geographic coordinates
geographic_area_name	The name of the geographic area covered by the present scenario hazard analysis. Can be used by a geocoder (e.g. geopy). The user can provide a comma-separated list of geographic names. [str]
creation_date	The date of creation (ISO 8601 format e.g. 2017-11-26, see https://en.wikipedia.org/wiki/ISO_8601). [str]
hazard_type	The typology of natural hazard modelled (controlled vocabulary) <ul style="list-style-type: none"> • Drought • Earthquake

	<ul style="list-style-type: none"> • Flood • Landslide • Storm surge • Tsunami • Volcanic eruption <p>[str]</p>
time_start	The time at which the modelled scenario(s) starts [ISO 8601 format]
time_end	The time at which the modelled scenario(s) ends [ISO 8601 format]
time_duration	The extent of the time period covered by the events included in the current scenario hazard analysis. [ISO 8601 format]
description	Used to provide general information about this specific scenario hazard analysis [str]
bibliography	A list of document names containing relevant information [str, ..., str]

2.6 “EVENT” ENTITY

The “Event” entity contains information about one specific scenario included in a given “Event Set”. Every “Event” instance will have the following attributes (the green background shows the attributes considered mandatory). The description is an important attribute and is where the event is described, for example in terms of magnitude.

Table 5 ‘Event’ entity attributes

Parameter	Description
id	A unique identifier [str]
event_set_id	The event_set.id parameter to which this event is associated. [str]
calculation method	The methodology used for the calculation of this event. This attribute is used to differentiate for example simulated events from observed events. Admitted options (controlled vocabulary): <ul style="list-style-type: none"> - Observed - Inferred (from observed data) - Simulated <p>[str]</p>

frequency	The frequency of occurrence of the present event (for the reference period see occurrence_time_span or occurrence_time_start and occurrence_time_end). [float, adimensional]
occurrence_probability	The probability of occurrence in a given time interval defined either through the occurrence_time_start and occurrence_time_end or through the occurrence_time_span parameter. [float, adimensional]]
occurrence_time_start	The start date (and possibly time) of the time period used to specify either the frequency or the occurrence_probability [ISO 8601 format]
occurrence_time_end	The end date (and possibly time) of the time period used to specify either the frequency or the occurrence_probability [ISO 8601 format]
occurrence_time_span	The duration of the period used to specify either the frequency or the occurrence_probability [float, years]
triggering_hazard_type	One value accepted for the event_set.peril_type attribute [str]
triggering_event_id	The identifier of a event (i.e. event.id) used as a trigger for the simulation of the corresponding footprints [str]
description	Used to provide general information about this specific event. E.g. in case of an earthquake with this attribute is possible to specify the magnitude of the earthquake or information about the rupture. [str]

2.1 “FOOTPRINT SET” ENTITY

The “Footprint set” entity contains a sub-group of the “Footprints” computed for an “Event”; all the “Footprint”s in a “Footprint Set” have the same unit of measure, represent the same process-type and their uncertainty is described in a homogenous way. Every “Footprint Set” instance will have the following attributes (the green background shows the attributes considered mandatory).

Table 6 ‘Footprint entity’ attributes

Parameter	Description
id	A unique identifier [str]
event_id	The event.id parameter to which this footprint is associated.

	[str]
process_type	<p>The typology of process modelled (controlled vocabulary).</p> <ul style="list-style-type: none"> • Drought • Earthquake: <ul style="list-style-type: none"> • Ground motion (e-gm) • Primary surface rupture (e-psr) • Secondary surface rupture (e-ssr) • Liquefaction (e-liq) • Flood <ul style="list-style-type: none"> • Water depth • Landslide <ul style="list-style-type: none"> • Rock fall • Debris flow • Storm surge <ul style="list-style-type: none"> • Inundation • Tsunami <ul style="list-style-type: none"> • Inundation • Volcanic eruption <ul style="list-style-type: none"> • Ash fall
imt	<p>Intensity measure types</p> <ul style="list-style-type: none"> • Drought <ul style="list-style-type: none"> ◦ SPEI • Earthquake: <ul style="list-style-type: none"> • PGA • SA(period) • Etc.
data_uncertainty	<p>This attribute defines the typology of uncertainty used for this specific event. Some potential options:</p> <ul style="list-style-type: none"> • Eventset [in this case the “Footprint Set” will contain many “Footprint”] • Equiprobable [in this case the “Footprint Set” will contain only one “Footprint”] • Normal • Lognormal

2.2 “FOOTPRINT” ENTITY

The “Footprint” entity contains information on a specific realisation of an “Event”. The uncertainty of a particular event is captured either by the construction of many footprints or by a single footprint which contains also information about uncertainty. Every instance will have the following attributes (the green background shows the attributes considered mandatory).

Table 5 ‘Footprint entity’ attributes

Parameter	Description
<code>id</code>	A unique identifier [str]
<code>footprint_set_id</code>	The <code>footprint_set.id</code> parameter to which this footprint is associated. [str]
<code>data</code>	A list of points used to describe the spatial distribution of a scenario. The coordinates of each point are in geographic coordinates (decimal degrees and WGS84 ellipsoid). This array has cardinality [m x 3] where the three columns represents longitude, latitude and intensity measure, respectively. ‘m’ corresponds to the number of points used. An [m x 3] array of floats
<code>data_uncertainty_2nd_moment</code>	A list of points used to describe uncertainty for the values in the <code>data</code> attribute. This array has cardinality [m x 3] where the three columns represents longitude, latitude and intensity measure, respectively. ‘m’ corresponds to the number of points used. An [m x 3] array of floats
<code>triggering_footprint_id</code>	The <code>id</code> (i.e. <code>footprint.id</code> attribute) identifying the footprint used as a trigger for the simulation of this footprint. For example, suppose the current footprint describes landslide permanent ground deformation triggered by an earthquake. In this case the value of this attribute will correspond to a list containing the id of the footprints describing ground shaking and shaking duration of the triggering event. list of [str]

2.3 UNCERTAINTY

The data schema supports different approaches to uncertainty which are expected as a result of the different hazard assessment methodologies. Options include:

- No uncertainty information. For example, Shakemap (USGS does provide uncertainty information but prototype code not currently able to import it).
- Text description. For example, ‘lognormal with sigma x’ (e.g. NGI Tsunami)
- Multiple footprints. For example GVM and GEM scenarios.
 - o Allows selection of individual simulations
 - o Allows extraction of mean and percentiles with SQL query
 - o Very resource intensive in terms of storage and processing.

2.4 DATA SCHEMA COMPILED EXAMPLE

We provide an example of usage of the proposed data schema below. Some further examples of the scenarios compiled during the project are given in Annex 1.

2.4.1 Case 1: A single observed scenario

We consider here the ground shaking produced by the L'Aquila earthquake (Central Italy) in 2009 as modelled in the USGS shakemap system.

Event Set

```

id - es1
geographic_area_bb - [13, 42, 13.4, 42.4]
geographic_area_name - L'Aquila, Abruzzo, Italy
creation_date - 2018-01-20
hazard_type - earthquake
time_start - 2009-04-06 01:32:39 UTC
time_end - 2009-04-06 01:32:39 UTC
time_duration - None
description - The L'Aquila earthquake (M6.3 according to the
USGS -
https://earthquake.usgs.gov/earthquakes/eventpage/usp000gvtu#executive) occurred on April 4th, 2009. The earthquake killed 309
persons and caused extensive damage to the city of L'Aquila.
Here we collect the shakemap for PGA produced by the USGS.
bibliography - None

```

Event

```

id - e1
event_set_id - es1
calculation_method - inferred
frequency - None
occurrence_probability - None
occurrence_time_start - 2009-04-06 01:32:39 UTC
occurrence_time_end - 2009-04-06 01:32:39 UTC
occurrence_time_span - None
triggering_hazard_type - None
triggering_event_id - None
description - None

```

Footprint set

```

id - fps1
event_id - es1.e1
process_type - ground shaking
imt - PGA
data_uncertainty - None

```

Footprint

```
id - fpl
```

```

footprint_set_id - es1.e1.fps1

data - A matrix with the following cardinality [4, 5, 3]

13,0, 42.1, 0.1
13,0, 42.2, 0.2
13,0, 42.2, 0.3
...
data_uncertainty_2nd_moment - None
triggering_footprint_id - None

```

2.4.2 Case 2 - Simulated earthquake scenarios for Dodoma.

In this second example, we describe the information collected about a number of simulated ground shaking scenarios for the city of Dodoma, Tanzania.

Event Set

```

id - es2
geographic_area_bb - [-9, 33, -3, 39]
geographic_area_name - Dodoma, Tanzania
creation_date - 2018-01-20
hazard_type - earthquake
time_start - None
time_end - None
time_duration - None
description - Simulated ground shaking maps for Dodoma, Tanzania
bibliography - Poggi, V., Durrheim, R., Mavonga Tuluka, G.,
Weatherill, G., Gee, R., Pagani, M., Nyblade, A., Delvaux, D.,
2017. Assessing Seismic Hazard of the East African Rift: a pilot
study from GEM and AfricaArray. Bull. of Earth. Eng.
doi:10.1007/s10518-017-0152-4

```

Event

```

id - e1
event_set_id - es2
calculation_method - simulated
frequency - 1/475
occurrence_probability - None
occurrence_time_start - None
occurrence_time_end - None
occurrence_time_span - None
triggering_hazard_type - None
triggering_event_id - None
description - The event considered is the one providing the
largest contribution to the hazard (expressed in terms of PGA)
with 10% probability of exceedance in 50 years (i.e. a return
period of 475 years). This event has a magnitude lower than 5.5
and a rupture-site distance shorter than 25 km.

```

Footprint set

```
id - fps1
event_id - es2.e1
process_type - ground shaking
imt - PGA
data_uncertainty - Eventset
```

Footprint

```
id - fp1
footprint_set_id - es2.e2.fps1
data - A matrix with cardinality [5, 3]
```

```
34, -8., 0.1
35, -7., 0.2
35, -6., 0.3
34, -5., 0.4
36, -4., 0.5
```

```
data_uncertainty_2nd_moment - None
triggering_footprint_id - None
```

```
id - fp2
footprint_set_id - es2.e2.fps1
data - A matrix with cardinality [5, 3]
```

```
34, -8., 0.3,
35, -7., 0.4,
35, -6., 0.8,
34, -5., 1.0,
36, -4., 0.9
```

```
data_uncertainty_2nd_moment - None
triggering_footprint_id - None
```

2.5 POPULATING THE DATABASE

In the next chapter we present the scenarios developed for each hazard to test the data schema and populate the proto-database. In some cases hazards analysis suffers from a lack of basic data for modelling (e.g. volcanic or tsunami hazard), or insufficient data to fully consider uncertainty (e.g. ground shaking in low seismicity areas) and yet it is clear that only a handful of events calculated using probabilistic approaches generate enormous amounts of data. The prototype import code has been found to be rather slow with binary formats and bulk data approaches more appropriate for large datasets.

3 Earthquake hazard scenarios²

3.1 INTRODUCTION

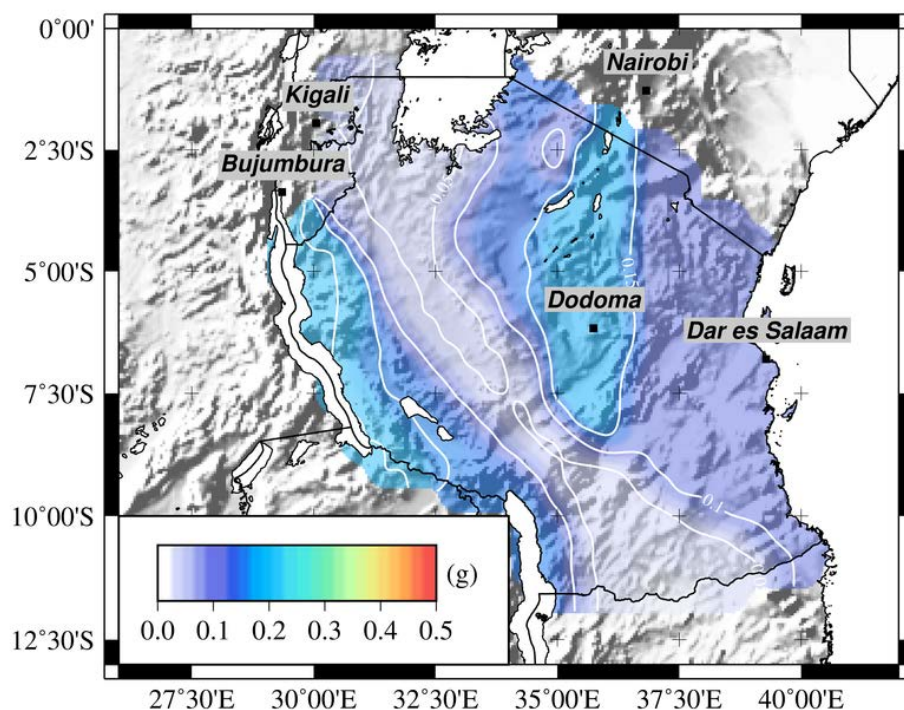
Given the paucity of observed earthquake events, for this analysis we opted for the generation of simulated scenarios starting from the information included in a regional long-term seismic hazard model. The reference hazard model selected is the one of Poggi et al. (2017) while the methodology adopted for the definition of the scenario relies on the selection of some reference intensity measure types (e.g. peak ground acceleration, PGA) and return period of interest (e.g. 475 years) and the execution of a seismic hazard disaggregation analysis. In the following section we illustrate the main characteristic of the seismic hazard model while in Section 3 we describe the disaggregation analysis performed and the main results obtained. In Section 4 we discuss the selection of the most plausible ruptures to be used for the calculation of ground shaking and finally in section 5 we describe the computed results.

3.2 PSHA RESULTS IN TANZANIA

For the calculation of the local earthquake hazard, we selected the probabilistic model for the East African Rift System (EARS) developed by GEM (Poggi et al., 2017) in collaboration with AfricaArray within the project SSHARA funded by US Agency for International Development (USAID). This hazard model was developed for the OpenQuake engine, the earthquake hazard and risk calculation engine developed by the Global Earthquake Model (Pagani et al., 2014; Silva et al., 2014). The model contains 19 homogenous area source zones describing spatial distribution and occurrence characteristics of the - so-called - distributed seismicity. To obtain a comprehensive characterisation of hazard, we performed seismic hazard calculations in Tanzania for different spectral accelerations (PGA and 0.05, 0.1, 0.2, 0.5, 1.0 and 2 seconds) and probabilities of exceedance (10% and 2% in 50 years). Example results can be seen in Figure 2 (hazard maps), Figure 3 (hazard curves) and Figure 4 (uniform hazard spectra).

² V. Poggi and M. Pagani, Global Earthquake Model Foundation

PGA)



Sa 0.2s)

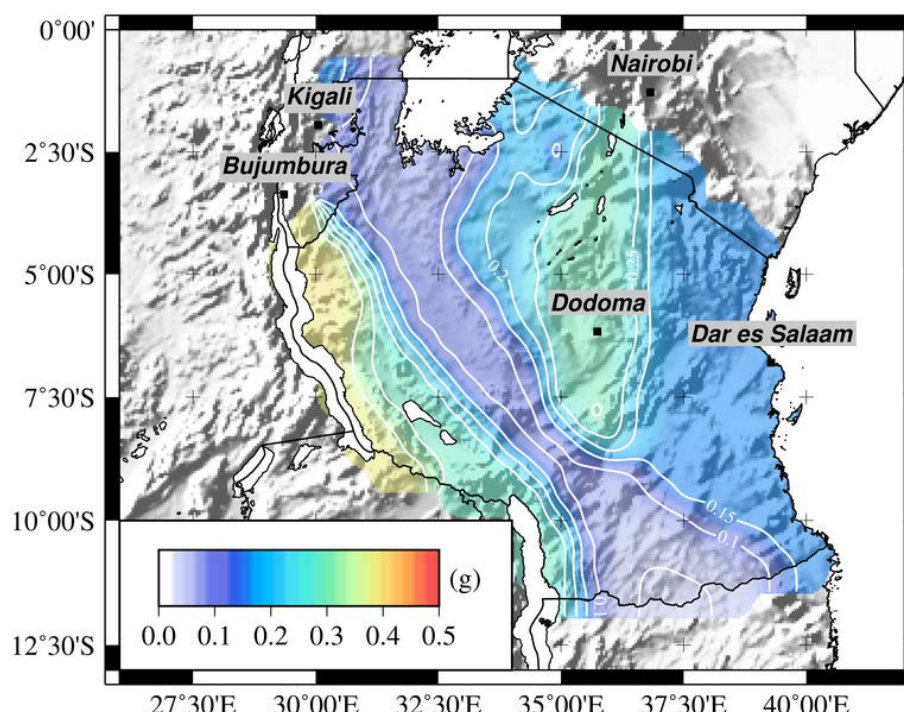
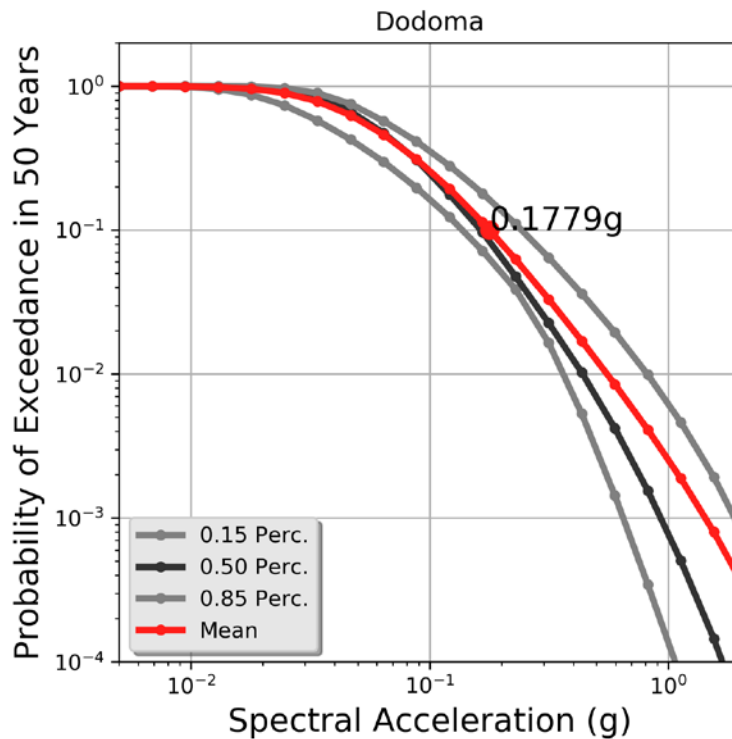


Figure 2 Probabilistic seismic hazard map computed for Tanzania using the model developed by Poggi et al. (2017). In this example, calculation is done for 475 years return period at PGA (top) and spectral acceleration at 0.2 seconds (bottom).

PGA)



Sa 0.2s)

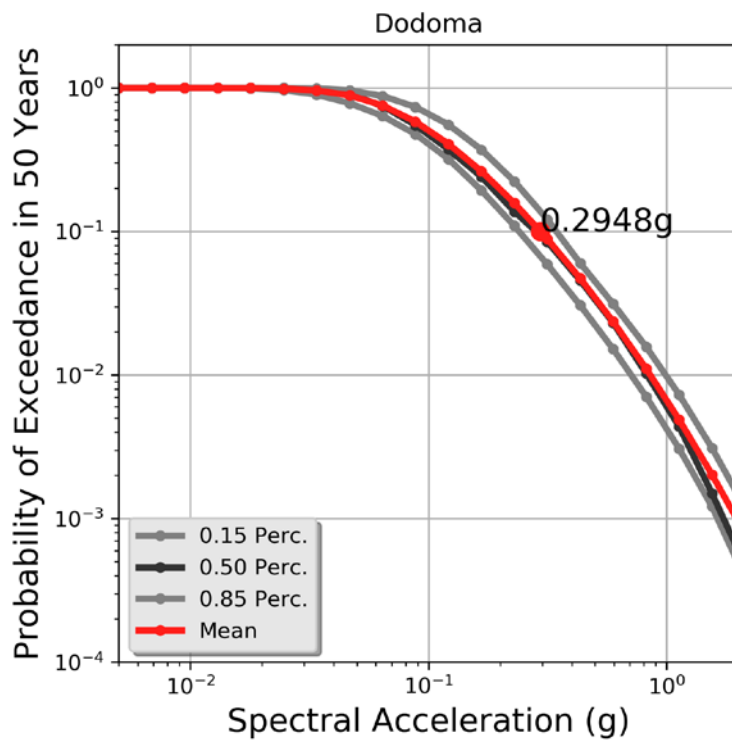


Figure 3 Hazard curves computed for the town of Dodoma (Tanzania) using the model developed by Poggi et al. (2017). In this example, calculation is done for 50 years investigation time at PGA (top) and spectral acceleration at 0.2 seconds (bottom). The value at 10% probability of exceedance is printed in each panel.

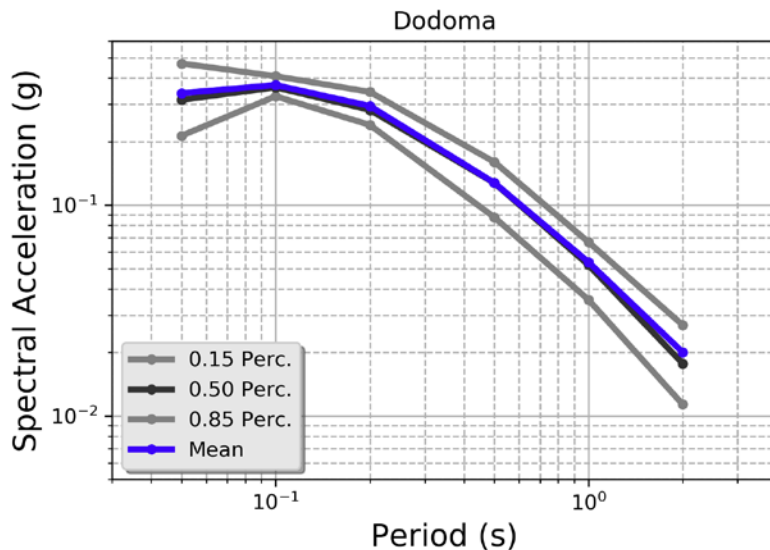
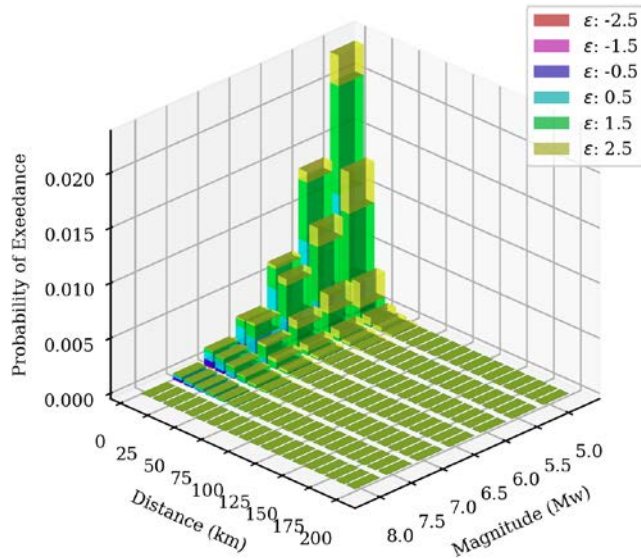


Figure 4 Uniform Hazard Spectrum (UHS) computed for the town of Dodoma (Tanzania) using the model developed by Poggi et al. (2017). In this example, calculation is done for 10% probability of exceedance in 50 years.

3.3 DISAGGREGATION

To define an earthquake scenario, disaggregation analyses have been performed. Disaggregation was computed for values of ground motion with 10% POE in 50 years using the results of the probabilistic seismic hazard analysis just described. In this study we performed seismic hazard disaggregation in terms of Magnitude-Distance-Epsilon (MDE) as well as in terms of geographical coordinates (Lat-Lon). It has to be mentioned that, by default, the disaggregation calculator provides a separated output for each end-branch of the implemented logic-tree. Mean disaggregation was then done a posteriori by averaging the probabilities from each branch realisation using weighted statistic (weights are computed from OpenQuake for each logic-tree end-member). Results for the MDE disaggregation at PGA (Figure 5 top) and spectral acceleration at 0.2 seconds are similar and show large sensitivity of the hazard to small magnitudes (<5.5) and close distances (<25km). For spectral acceleration at a period of 1 second ($Sa(1.0s)$; see Figure 5 bottom) the major contributions to hazard come from ruptures with larger magnitudes (between about 5.5 and 6.5) located at intermediate distances (>50km). This result is also confirmed by the geographic disaggregation results (Figure 6 top). In particular, for Sa at 1 second the influence of the larger distances is more evident along the direction NE-SW for the larger magnitudes (Figure 6 bottom for magnitude 7.5), which have nonetheless lower contribution to the hazard.

PGA)



Sa 1.0s)

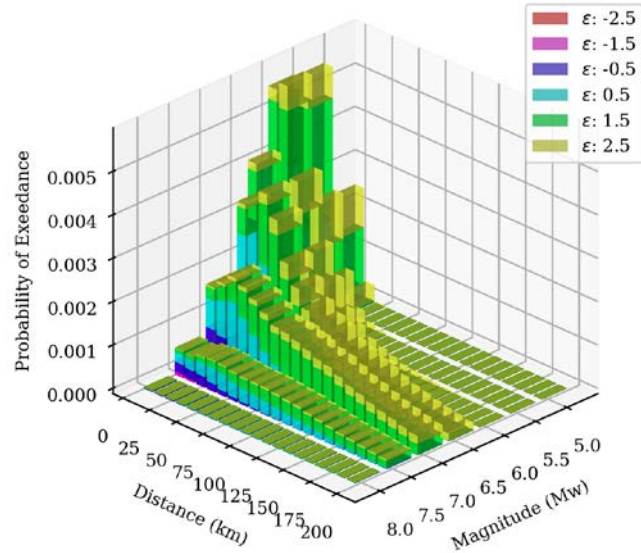


Figure 5 Mean disaggregation Magnitude-Distance-Epsilon computed for PGA with 10% probability of exceedance in 50 years (top) and spectral acceleration at 1 second with 10% probability of exceedance in 50 years (bottom).

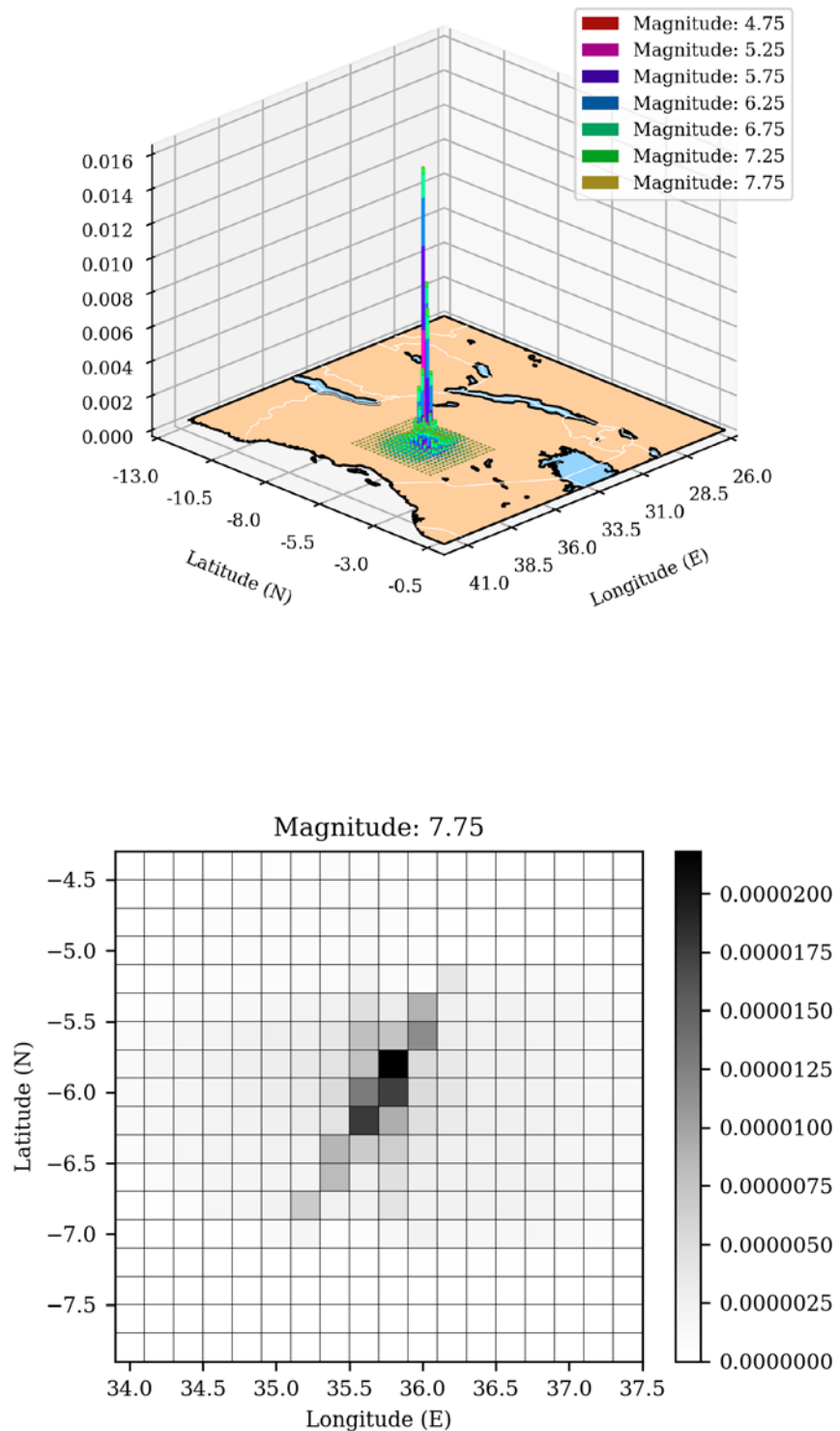


Figure 6 Mean geographical (Latitude-Longitude) disaggregation computed for spectral acceleration at 1 second with 10% probability of exceedance in 50 year, showing the contribution of different magnitudes; in the bottom panel we present the case for magnitude 7.75, which shows a particularly pronounced directionality (less pronounced at lower magnitudes).

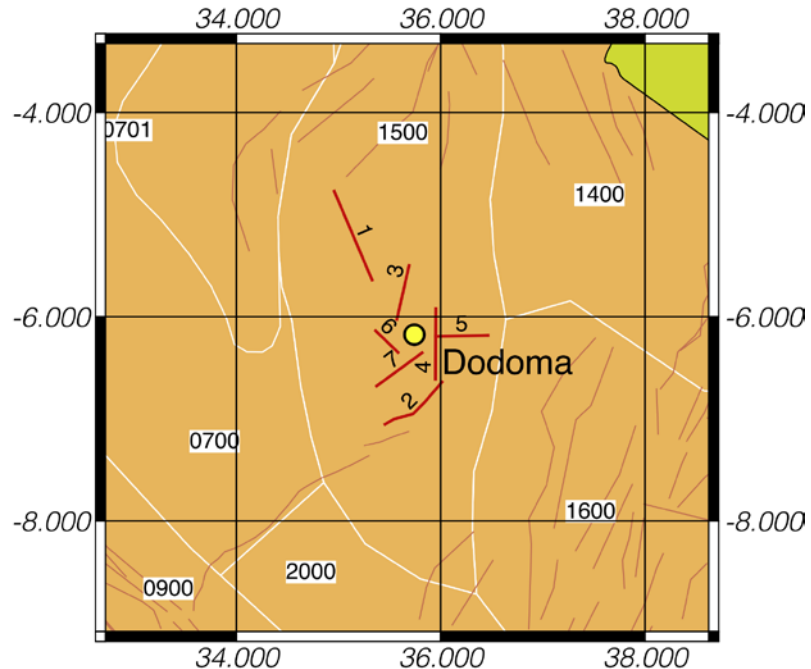


Figure 7 Orientation of the 7 faults assumed compatible with the hazard scenario from disaggregation of the Dodoma region. We plot in the background the fault dataset of Macgregor 2015 (thin red lines) and the area source zones included in model of Poggi et al. 2017.

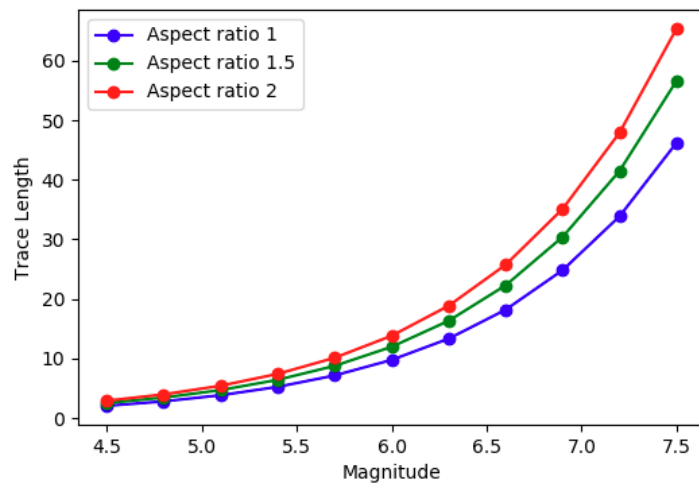
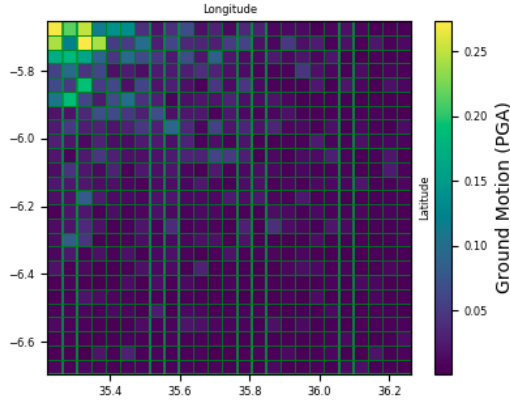
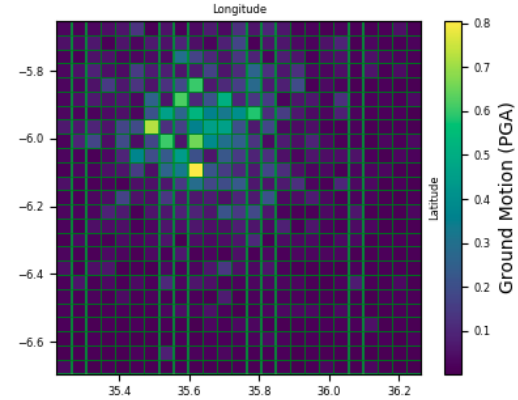


Figure 8 Rupture trace length as a function of magnitude computed using the Wells and Coppersmith (1994) scaling relation and three different aspect ratios.

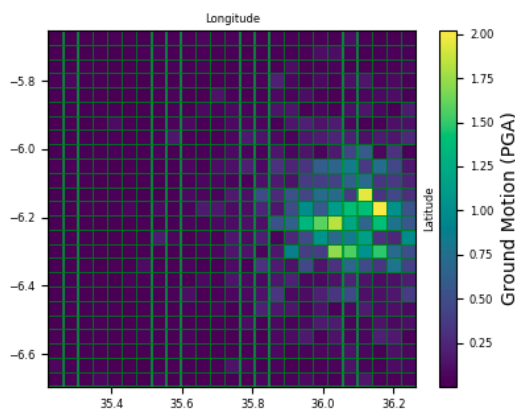
A) Fault 1



B) Fault 3



C) Fault 5



D) Fault 7

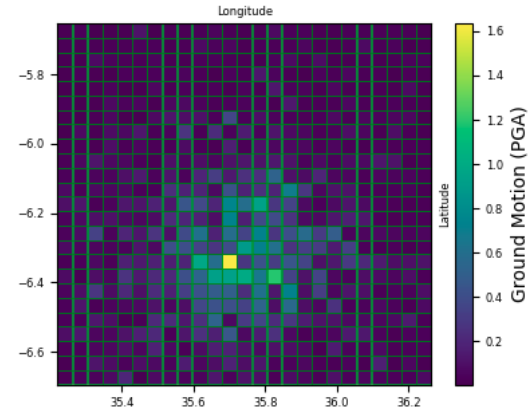


Figure 9 Example of ground motion field computed in the area of Dodoma for different the faults. Although the simulated magnitude scenario is identical between realizations (M 6), the absolute value of the ground motion is noticeably different due to the different sampling of the GMPEs uncertainty.

3.1 FAULT SCENARIO DEFINITION

Given the results of the disaggregation analysis for Dodoma, we decided to define a set of scenarios compatible with a magnitude 6 and distance between 10 and 25km. Seven faults were then selected/created in the region surrounding the city. Two observed faults from the database of Macgregor (2015) have been considered (fault 1 and 2) as potentially compatible of the identified scenario from disaggregation. Other 5 faults have also been hypothesized closer to Dodoma than the two observed and assuming orientation and geometry compatible with the rupture mechanisms prescribed by the SSHARA model for zone 15-00. While dip has always been kept constant for all sources (60° , assumed typical value for faults in a normal stress regime), rake was assigned either -90° (normal; faults 2, 3, 4, and 6) and -45° (normal with strike-slip component; faults 1, 5 and 7). Additionally, maximum trace length of each fault has been scaled to match the rupture extension generated by a magnitude 6 event. For that, we used the Wells and Coppersmith (1994) scaling relation, assuming an aspect ratio of 1.5 (Figure 8).

3.2 GROUND MOTION FIELD SIMULATION

For each fault source, 100 stochastic ground motion field simulations have been computed separately for each GMPE logic-tree end-branch (Figure 9) of the original model, with the only exception of Atkinson and Boore (2006), that has been discarded due to the unexpectedly high ground motion predicted around the epicentre. For that reason, such GMPE is presently under verification. Calculations were done at PGA and spectral acceleration 0.2s and 1s, for a grid of 25*25 points with spacing of about 0.042 degrees centred on Dodoma (35.741944, -6.173056).

4 Volcanic ash fall hazard scenarios³

4.1 INTRODUCTION

In this chapter we outline the methods and parameters used in simulating tephra fall footprints for three eruption scenarios of relatively low, medium and high probability at Rungwe volcano, Tanzania. We chose Rungwe volcano because it is one of the better studied volcanoes in sub-Saharan Africa, and was the focus of an expert elicitation on frequencies as part of a World Bank GFDRR project in 2015-2016. Rungwe is not one of the more frequently active volcanoes in Tanzania but it poses a risk in the southern part of the country. Ol Doinyo Lengai in the north has erupted frequently since 1900AD causing damage to vegetation, killing livestock, causing injuries among the Maasai, and impacting the tourism sector. As a result, there is increased awareness of volcanic risk in the north of Tanzania.

4.1.1 Terminology

Volcanic Explosivity Index (VEI) - a relative scale that enables explosive volcanic eruptions to be compared with one another. It is based on the volume of explosive ejecta, eruption cloud height and other observations.

Volcanic tephra – tephra is the fragmented material formed during an explosive eruption, fragments may be any size or composition. In this chapter we refer to ‘tephra’ as we have modelled a wide range of particle sizes.

Volcanic ash – often used to refer to all explosive eruption products (tephra) but strictly speaking volcanic ash fragments are less than 2mm in diameter.

Volcanic vent – the opening in the Earth’s crust through which an eruption takes place.

Eruption column – the ascending cloud of eruption debris above a vent, for larger more powerful eruptions it is vertical.

4.2 CHOSEN VOLCANO

All volcanoes in sub-Saharan Africa, including Tanzania, are characterised by poor data availability regarding their eruptive history, in other words the field studies needed to gather appropriate data for volcanic hazards have not yet taken place in sufficient detail at most volcanoes. As past activity is our best indicator of the likely future activity at a volcano, this poses a problem for hazard assessment.

There are ten volcanoes in Tanzania (Figure 10) located on the rift zone, Rungwe volcano is situated in the south of the country. We simulated tephra fall for Rungwe volcano as it is one of the better studied volcanoes in sub-Saharan Africa, and it has a record of VEI 4 and 5 eruptions (large explosions) in the Holocene (last ~10,000 years). In general, it is assumed that volcanoes active in the Holocene will erupt again in the future (www.volcano.si.edu). More than 2.3 million people live within 100 km of the volcano.

³ S. Jenkins, Earth Observatory of Singapore and S. Loughlin, BGS for the Global Volcano Model network.

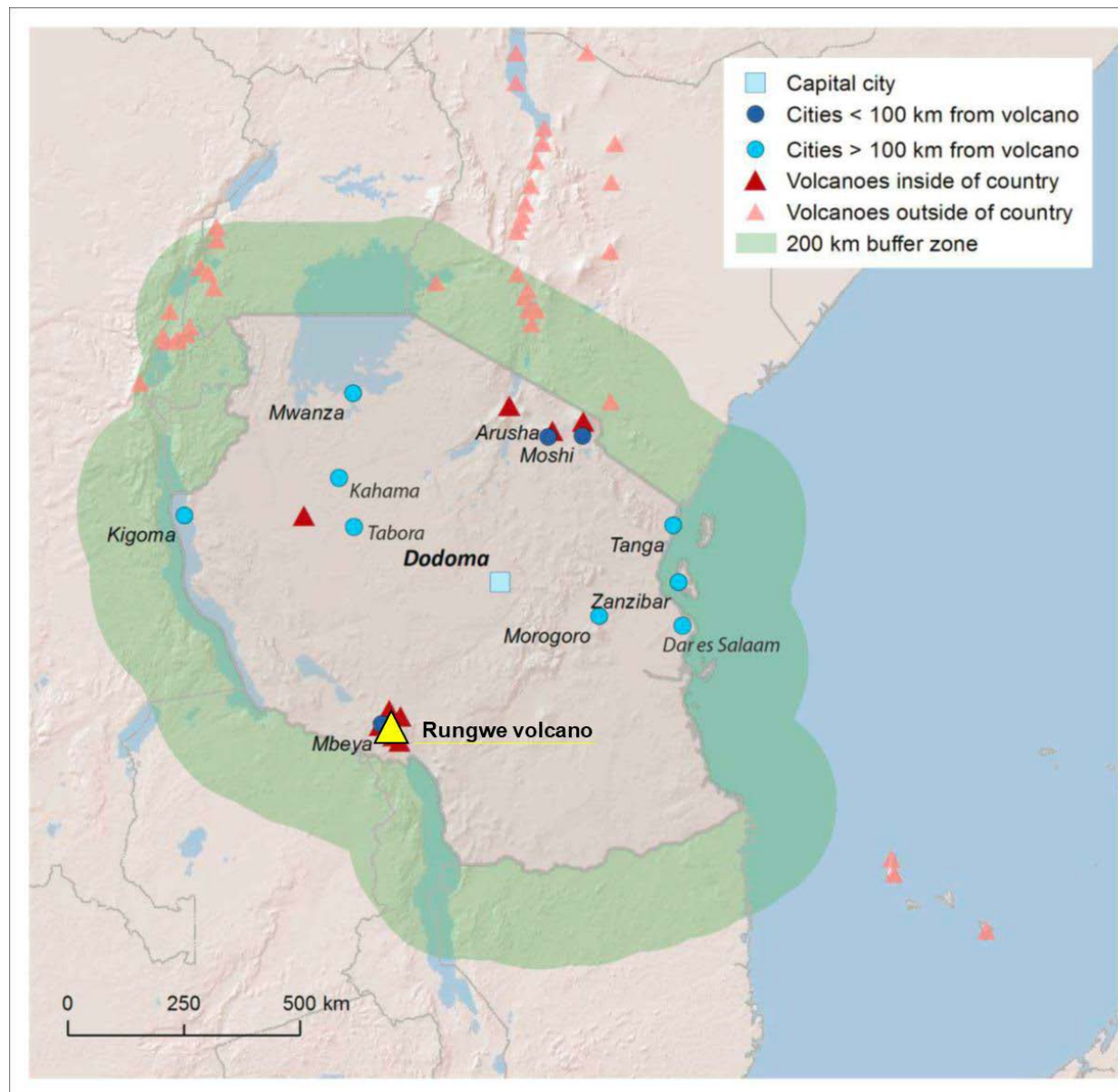


Figure 10 Holocene volcanoes within Tanzania (taken from the Global Volcanism Program www.volcano.si.edu), with the capital cities and study volcano highlighted (modified from Brown et al., 2015).

4.3 ERUPTION SCENARIOS

We have defined three scenarios specifically at Rungwe volcano of relatively low, medium and high probability:

VEI 2: A relatively small explosive eruption. The caldera and northwest flanks of Rungwe have numerous small cones that are indicative of relatively small tephra-producing eruptions of the order VEI 2.

VEI 4: A moderate large-magnitude explosive eruption as occurred at Rungwe in 50 years BCE (Isongole pumice).

VEI 6: A very large explosive eruption, with associated lower probability. While Rungwe does not have a documented record of a VEI 6 eruption, other volcanoes within the East African Rift Valley have produced such eruptions in the past. Many neighbouring volcanoes exhibit large calderas as evidence of major explosive eruptions, and the production of siliceous trachydacite

magma at Rungwe volcano suggests that a larger magnitude eruption is possible. We therefore include a VEI 6 eruption as a realistic worst case scenario *at this volcano*.

We believe these scenarios cover the range of future expected explosive behaviours *at this volcano* with return periods of between 450 and 3,000 years.

We have generated 1,000 footprints for each scenario to account for varying meteorological conditions and credible eruption source parameters. The footprints for Rungwe have the format: Easting, Northing, tephra load (kg/m^2) for UTM zone 36 south.

Tephra falls are expected to impact communities to the west of the volcano more than the east because of the wind conditions at the volcano. Dry and windy conditions in the region may promote remobilisation of the finer volcanic ash, which can produce repeated ash falls and disruption over years.

In the absence of detailed information and studies, and the time to carry out geological and geochronological studies, we rely on previous published geological studies, and a 2015-2016 study for the World Bank GFDRR, where we formally elicited the judgement of four experts familiar with East African Rift volcanoes with regards to likely future eruption characteristics at Rungwe. The elicitations aimed to provide source parameters for tephra fall modelling at select volcanoes in Ethiopia (Aluto, Corbetti, Fentale) and Kenya (Menegai, Longonot, Suswa) and used Rungwe in Tanzania as an analogue. The elicited eruption frequency-magnitude relationship is shown in Figure 11. A $\text{VEI} \leq 2$ can be considered of the same approximate return period as a $\text{VEI} 2$ (~450 years).

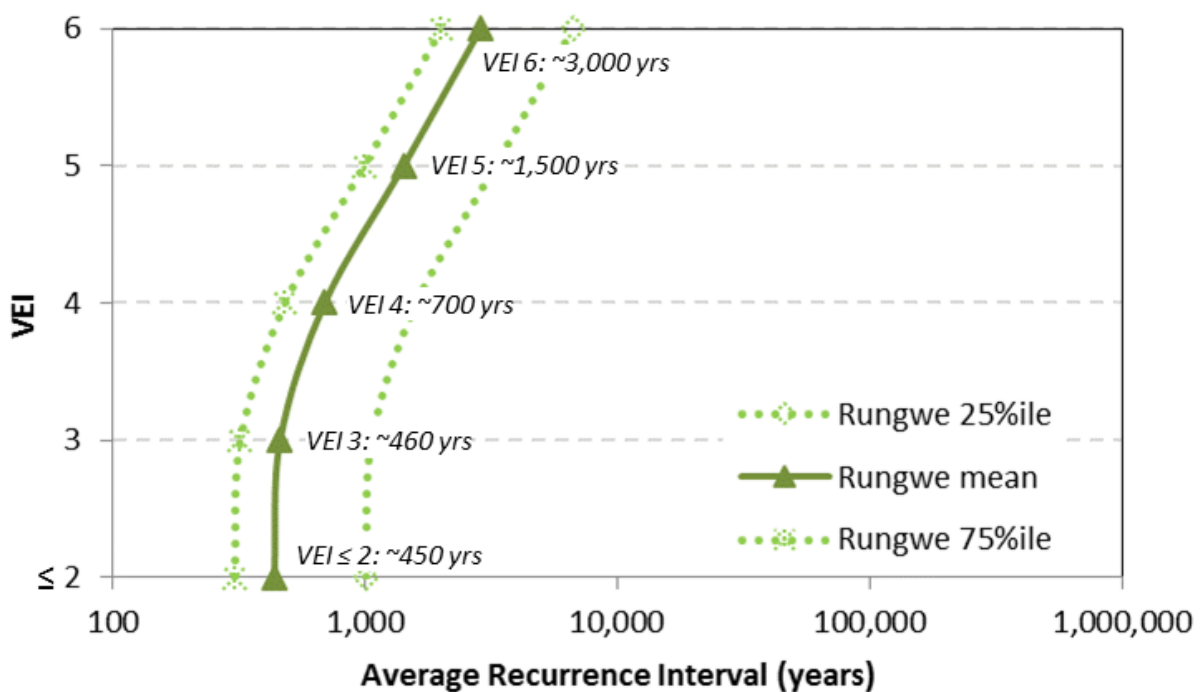


Figure 11 Frequency-magnitude relationship for Rungwe, which acted as an analogue for Fentale, Longonot and Suswa volcanoes, derived through expert elicitation. The solid line represents the mean estimate and the dashed lines the interquartile confidence bounds.

The eruption frequency-magnitude relationships are indicative of likely activity, but there are a number of limitations that mean they are subject to uncertainty as the eruption history at Rungwe is very limited. The eruption frequency is therefore a conservative estimate, given the paucity of data.

4.4 METHOD, METADATA AND RESULTS

We used TEPHRA2 (Connor et al., 2008), an analytical 2D tephra dispersal model to simulate a large range of potential eruption and wind conditions for each of three eruption scenarios. Simplistic 2D models of tephra dispersal and fall assume uniform wind conditions with distance and time horizontally away from the vent. At very long distances (100s of kilometres), and for very fine ash particles, i.e. for the purposes of aviation hazard assessment, these models are less reliable than their 3D counterparts; however, they are better suited for probabilistic modelling and have proven reliable in forecasting tephra deposit thicknesses (e.g. Carey and Sigurdsson, 1986; Komorowski et al., 2008). Each simulation produces a spatial distribution of tephra fall load. The columns are Easting, Northing, tephra fall load (in kg/m²) on a 5000 m by 5000 m grid. The UTM zone is 36 South.

4.4.1 Meteorological conditions

The distance and area over which tephra is dispersed is strongly controlled by varying wind direction and speeds at different altitudes and with distance from the vent. Wind conditions were sampled randomly from a ten-year record of reanalysis data (ECMWF ERA-Interim: 2005-2014) at six-hourly intervals, interpolated to 1 km height intervals above the vent. For each eruption scenario, we modelled 1000 different simulations to account for varying wind conditions and source parameters. The averaged wind directions and speeds at Rungwe volcano are shown in Figure 12, as a function of height above the surface and by month to show seasonal effects.

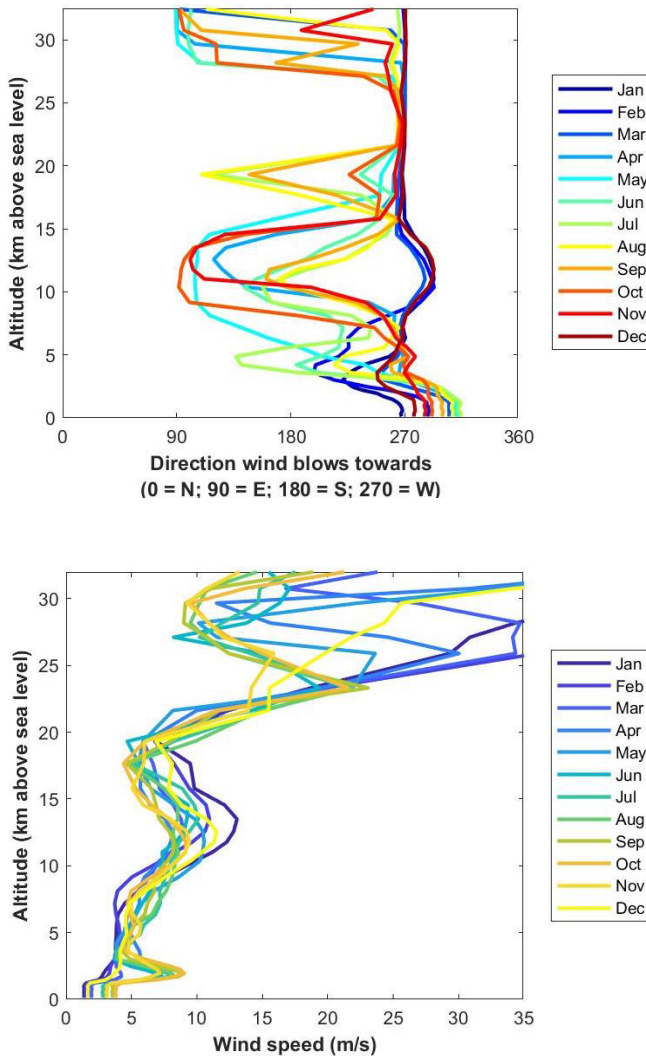


Figure 12 Wind direction (left) and speed (right) averaged by month, with height above surface, for the ECMWF ERA-Interim 6 hourly reanalysis data used in this study (2005-2014).

4.4.2 Particle characteristics

An important influence on how far tephra will be dispersed is the size and density, and thus settling velocity, of the erupted particles. Such characteristics are influenced by the magma composition, presence of water, eruption style and weather conditions.

Particle size

A normal distribution (on a phi scale) of grain sizes is used, with bounds 4 phi (63 microns) and -5 phi (32 mm), with a median between -1 and -3 phi and standard deviation of 1.5 to 2.5 phi, following the total grain size derived by Fontijn et al. (2011) for the VEI 4 Rungwe pumice produced ~4,000 years ago. It was assumed that the fine material would either fall as aggregates captured within these grain size bounds, or be dispersed much farther than the ash fall footprints being simulated.

Particle density

An averaged particle density of 680 kg/m^3 was used. This estimate was achieved by considering a lithics:pumice proportion of 10:90 following data from Kone, Aluto and Rungwe volcanoes, although it was recognised that data are from proximal to medial deposits and so may overestimate

the proportion of lithics. Lithics are expected to be mostly trachytes or syenites (Rungwe: 2300 kg/m³). Pumices are expected to have densities of around 500 kg/m³ (Rungwe: Fontijn et al., 2011).

4.4.3 Erupted tephra volume

We sourced the bulk erupted volume from the VEI classification for each eruption scenario (Newhall and Self, 1982); however, the VEI classification includes all erupted pyroclastic material. A VEI 6 eruption was assumed to be caldera-forming so that much of the volume would collapse into pyroclastic density currents, rather than remain in a sustained tephra column. Following discussions carried out as part of the 2015-2106 elicitation, the proportions and volumes of tephra that may be dispersed in the atmosphere for each scenario are shown in Table 7. The volume was converted to mass assuming the derived particle density of 680 kg/m³.

Eruption scenario	Proportion tephra	Bulk volume (km ³)	Mass (kg)
VEI 2	100%	0.001 to 0.009	6.8×10^8 to 6.7×10^9
VEI 4	100%	0.1 to 0.99	6.8×10^{10} to 6.7×10^{11}
VEI 6	50%	5 to 49.99	3.4×10^{12} to 3.4×10^{13}

Table 7 The proportion of the explosively erupted material that is dispersed in the atmosphere as tephra (as opposed to collapsing as pyroclastic density currents).

4.4.4 Eruption column height

The height to which tephra is erupted above the volcanic vent is calculated from the erupted volume using the empirical relationship derived by Jenkins et al. (2007) for explosive eruption stages:

$$\text{Height (km)} = 8.67 \cdot \log_{10}(\text{Volume in km}^3) + 20.2$$

This relationship is similar to that of Carey and Sigurdsson (1989) for Plinian volumes but does not require conversion from mass to volume. Both assume a sustained plume with no effect from wind on the plume height as the relationship is for larger VEIs. For VEI 2, we assume column heights of between 1 and 5 km, following Newhall and Self (1982).

Table 8 The height of the erupting column above the volcanic vent for each scenario.

Eruption scenario	Column height
VEI 2	1 to 5 km
VEI 4	11.5 to 20 km
VEI 6	26 to 35 km

4.4.5 Other parameters

We assumed the following values for additional parameters required by TEPHRA2:

- Fall-time threshold: 10,000 seconds; to permit finer grains to fall out.
- Plume ratio: 0.8; tephra mass is concentrated in the upper 80% of the column.
- Eddy constant: 0.04 m³/s; Value for Earth for small particles.
- Diffusion coefficient: 3000 m²/s.

For each eruption scenario, we ran 1000 simulations on varying grid extents (larger grids for larger VEIs) with a uniform spatial resolution of 5 km².

4.4.6 Results

The results of the simulations as demonstrated at the workshop in Tanzania are shown in Figures 13-15. For each of the three scenarios, there were 60M data points in total which has significant implications for visualisation and use.

1 Event Set containing:

3 Events (1/450, 1/750, 1/3000 years) each containing

1 Footprint set (tephra-load, kg/m²) containing

1000 Footprints each containing between 7,000 and 36,000 intensity values.

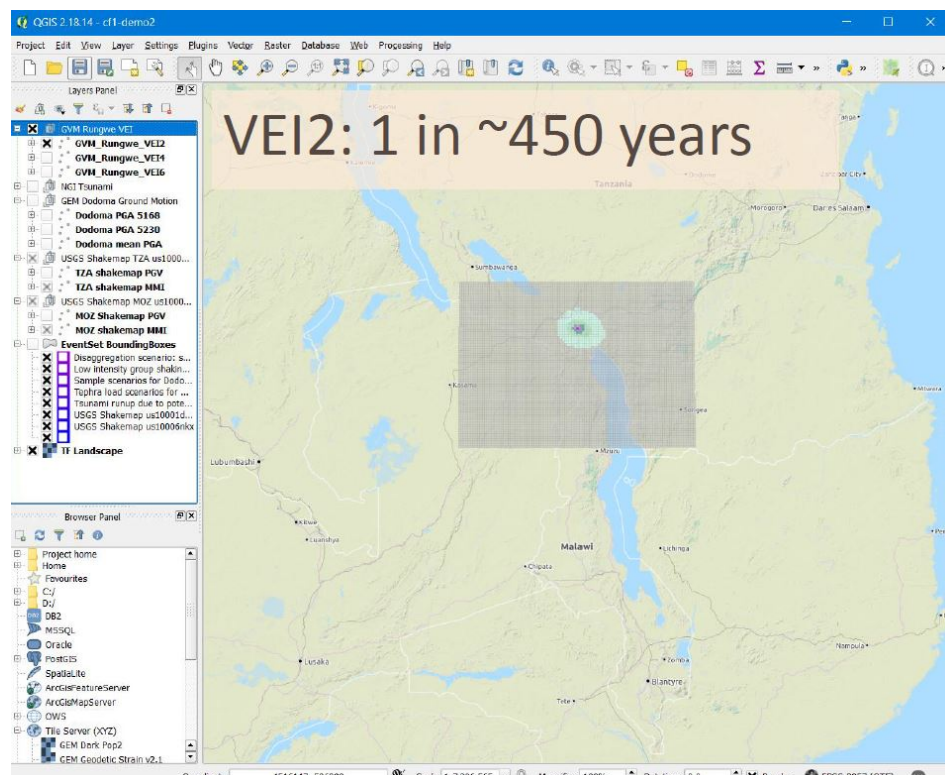


Figure 13 The hazard footprint for a VEI 2 explosive eruption scenario at Rungwe volcano.

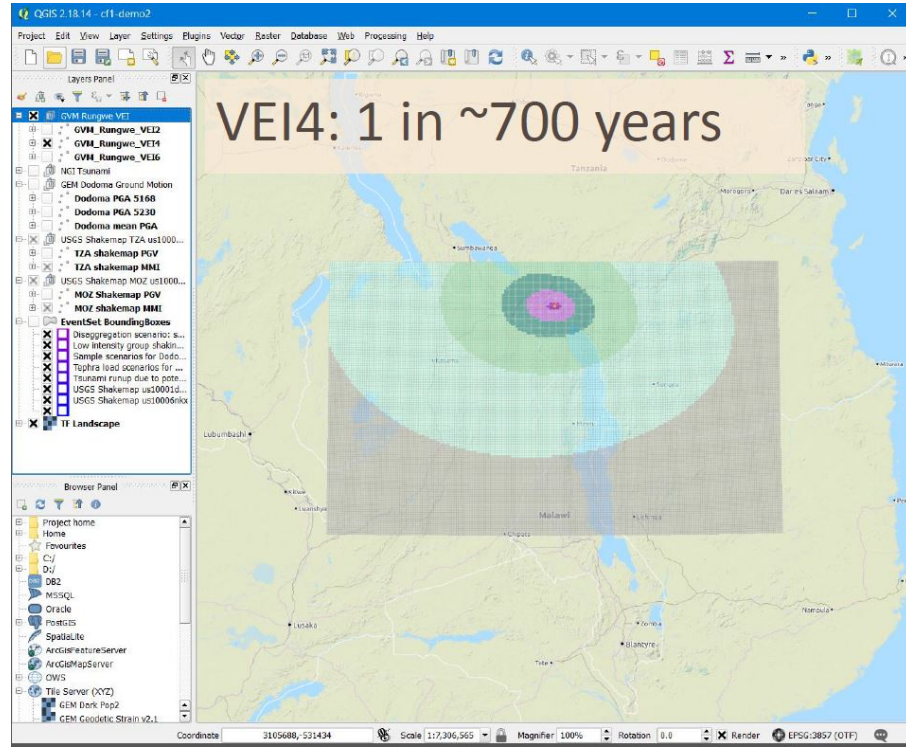


Figure 14 The hazard footprint for a VEI 4 explosive eruption scenario at Rungwe volcano.

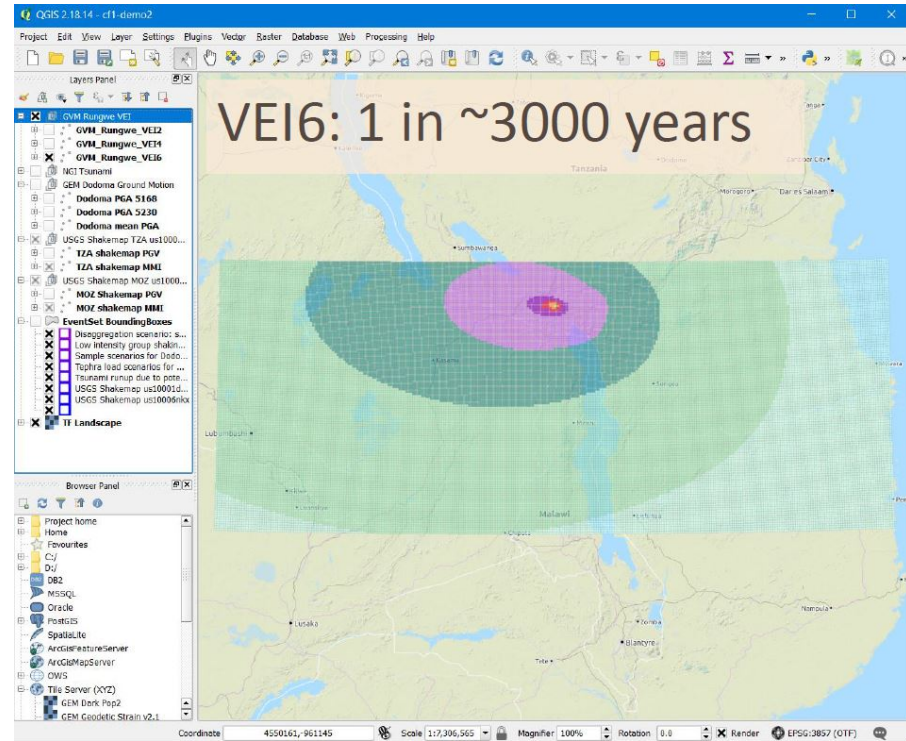


Figure 15 The hazard footprint for a VEI 6 explosive eruption scenario at Rungwe volcano.

4.5 SUMMARY

4.5.1 Guidance on use

There are a number of limitations associated with probabilistic modelling of tephra fall:

- These scenarios are based *on just one volcano*, ideally modelling would be carried out for other more frequently active volcanoes such as Ol Doinyo Lengai (seventeen eruptions since 1900AD) and Meru (two eruptions since 1900AD) if sufficient data and expertise can be compiled.
- The hazard to aviation and from wind remobilisation of deposits is not accounted for with our modelling. Impacts to aviation are expected to affect much larger areas (in the case of airborne ash), and continue for months, years or even decades (in the case of remobilisation).
- A future eruption at Rungwe volcano is unlikely to have exactly the source parameters modelled here; for example, the particle size can be strongly influenced by the magma composition or the presence of water and a finer particle size distribution will lead to a larger area being impacted.
- 2D tephra dispersal models typically overestimate very proximal (<5 km) deposits. Given the near complete devastation that may be expected with tephra falls of 1 m or more (Jenkins et al., 2015), this may be used as a reasonable upper bound.

4.5.2 Future improvements

Tanzania is suffering the impacts of volcanic activity on a regular basis as a result of the frequent eruptions of Ol Doinyo Lengai, but the impacts of these eruptions primarily on the Maasai are poorly documented (De Schutter et al. 2015).

In terms of improvements for the future, further geological fieldwork is very important at Tanzania's active volcanoes to establish, at least in outline, a geochronological eruption history for the volcanoes. In addition, geological mapping can establish the most likely styles of eruptive activity and types of hazards.

Ideally, a national scale assessment of volcanic tephra fall hazard would be carried out using a combination of new field data, analogue volcanoes and expert elicitation.

4.5.3 Impacts and comparison with other hazards

Volcanic eruptions can demonstrate unrest (signs of magma moving towards the surface) long before an eruption. These signs can result in the self-evacuation of populations if the signs are alarming (e.g. felt earthquakes, gas emissions). When an eruption begins it can last weeks (global average eruption duration is ~7 weeks) to years. In the longer term, displacement of populations, loss of livelihoods, and wide disruption (including to aviation and economy) are typical of volcanic eruptions, showing some similarities with drought and even flooding.

5 Landslide hazard scenarios⁴

5.1 INTRODUCTION

This chapter describes the development of landslide scenarios in a part of the Kilimanjaro region in north-east of Tanzania. The scenarios described include debris flows as a consequence of an extreme rainfall event in the region in question.

There exists limited information about the landslide activity in Tanzania. In a paper from 2017, Tegeje and Kervyn (2017) presented a review of spatial and temporal distribution of landslides in Tanzania. In that study, a total of 45 landslides were identified and mapped over a span of 106 years in Tanzania. Based on the number of landslide events, the north-eastern zone (NEZ) reported more events than other zones in the country and this is the area of most concern to colleagues at the Geological Survey of Tanzania (around Moshi). In terms of landslide types, this zone reported more mudslides/flows, debris flow and debris avalanches than other zones. In almost all the inventoried landslides, long duration of rainfall with varying intensities prior to the event was perceptually reported to trigger the event. Heavy precipitation is also cited as the main trigger for landslides in Tanzania. The NEZ is a highland area with more than 1500 mm of rainfall per year, with more rainfall received between November/December and April each year.

5.2 SCENARIO METHODOLOGY

In addition to the above information, the scenarios were based the evaluation of landslide susceptibility (spatial propensity to landslide activity) maps made for whole Tanzania. The methodology for the construction of the susceptibility maps was based on the model developed by NGI in previous projects (Dilley et al., 2005; UNISDR, 2009; NGI, 2009). In this model, the landslide susceptibility depends on four factors: topography, lithology, vegetation cover and soil moisture.

For the topography data, Digital Elevation Models (DEMs) were derived from one of two datasets: either the Shuttle Radar Topography Mission (SRTM) or Advanced Spaceborne Thermal Emission and Reflection Radiometer (ASTER). The SRTM dataset has 1 arc-second resolution (approximately 30 m), the higher resolution of the two datasets, but it also contains many voids. These occur primarily in ravines and highland areas, especially in the upper reaches of Mount Kilimanjaro. ASTER lacks these gaps, but many of these filled voids contain unrealistic artefacts.

Lithology information was downloaded from the Geological Survey of Tanzania's Geological and Mineral Information System. While documentation on which sources were compiled to construct this dataset is lacking, the dataset was deemed credible since it is from an official Tanzanian government website and that it is in agreement with other datasets that are only viewable in web portals (for example, <http://onegeology-geonetwork.brgm.fr/geonetwork3/srv/eng/catalog.search?node=srv#/metadata/cdba0dae32448f05425030ced2f77789832a9111>). The dataset is intended for use at a scale of 1:2,000,000.

Vegetation cover was not included in the determination of landslide susceptibility. While data from the Africa Land Cover Characteristics are available on a 1 km resolution, there is a lack of research on how to classify high- and low-susceptibility land use types in this region. Given the small relative effect of land use on landslide susceptibility compared to other factors, it was not included in this analysis.

⁴ F. Nadim, Norwegian Geotechnical Institution (Global Landslide Model)

Figure 16 presents the susceptibility map for whole Tanzania where S_r is slope factor, S_l is lithology factor and S_h is soil moisture factor.

$$S_{\text{landslide}} = S_r \times S_l \times S_h$$

In this model, S_r , S_l , S_h have ranges of 0-5, 1-3, and 1-3, respectively. $S_{\text{landslide}}$ is a subjective, relative susceptibility index that varies between 0 (no susceptibility to landslide) to 45 (high susceptibility to landslide).

The next step for developing a landslide scenario was to perform a similar study for the area in the Kilimanjaro region with high susceptibility. Figure 17 presents the susceptibility map for an area north of the main town, Moshi, in the Kilimanjaro region.

In Figure 18 a few watersheds are identified in the landslide-susceptible region north of Moshi. Out of these watersheds shown in Figure 18, we find W3, W2, W4, and W10 to be especially prone to debris flows given that they have the largest area and highest proportion of susceptible slopes. In these basins, given that the lithology (described by S_l) and soil moisture condition (S_h) remain constant at the resolutions available, the high hazard areas (and probable trigger zones) are taken as the locations with $S_r \geq 4$.

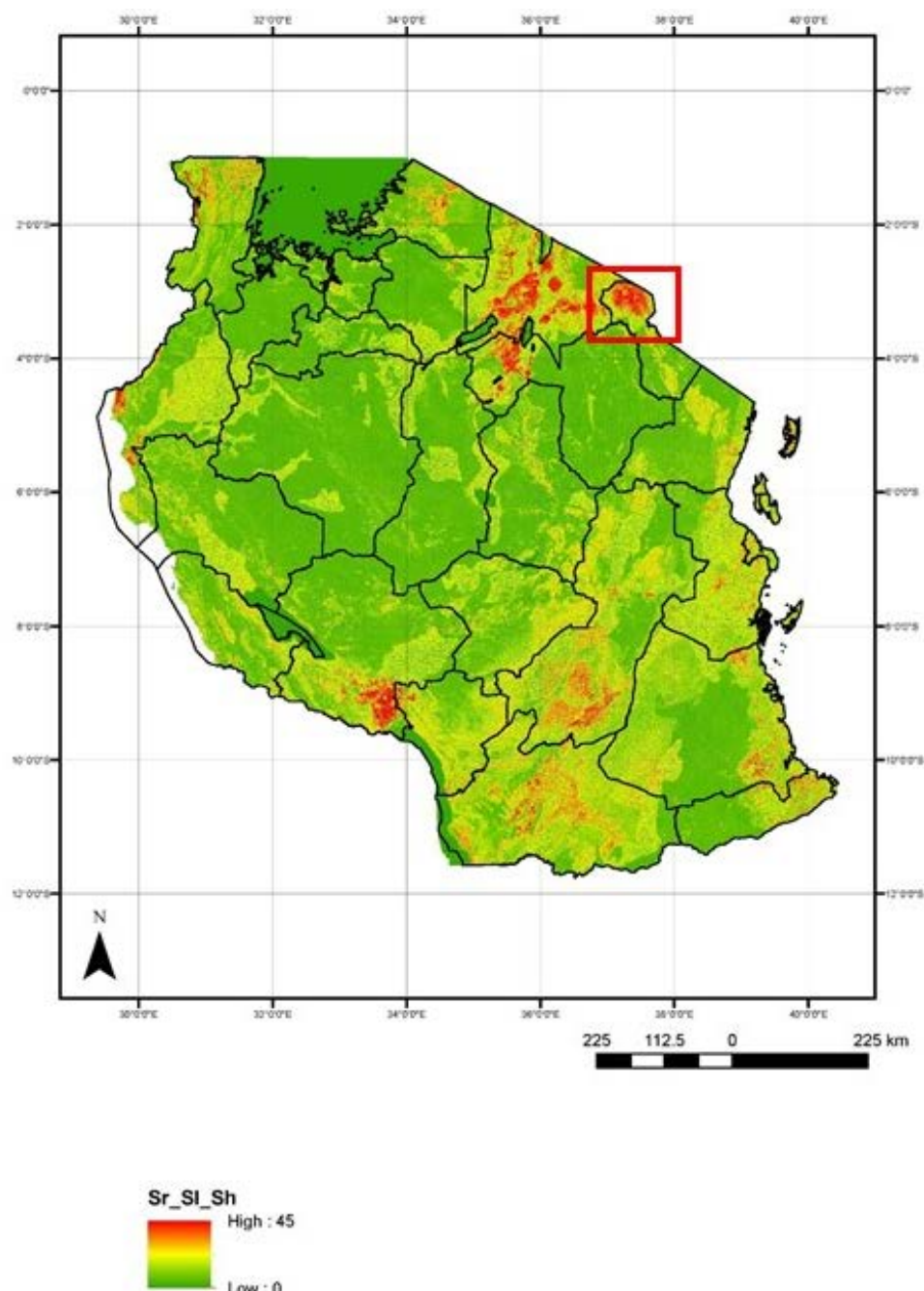
Runout distance was estimated using an empirical relationship developed by Rickenmann (2005) shown in Figure 19. The volume of a potential debris flow was estimated by taking 1% of the high hazard areas within each basin and multiplying it by a depth of 2 m. The estimated volumes are shown in Table 9.

Rickenmann's model suggests as a conservative estimate for that volume of flow, the runout distance (L) should be 10 times the drop in elevation (Δh). The difference between the mean elevation of high hazard cells within a basin and the elevation of the outlet was used as the value for Δh . The runout distance L was mapped starting from the mean position of high hazard cells within the basin. Figure 20 and Figure 21 show the runout areas for these watersheds. (No footprint is shown for W2 because the estimated runout was too short to reach the bottom of the longer basin.) The geographical data sets for these scenarios were provided for the proto-database.

Users of these maps must be aware of the limitations of the runout estimation method. The historical events that Rickenmann (2005) used were not from Tanzania, and the range of typical runout distances may differ in the Tanzanian context. Furthermore, in this case, debris flows have been assumed to follow existing water channels, and a minimum 400 m wide zone has been drawn perpendicular to these channels. However, this method assumes the volume of material is not sufficient to overtop the banks of these ravines. A number of simulations with an advanced 3-D numerical model for runout of debris flows would be required to predict the lateral extent of a flow more accurately.

Table 9 Estimated debris flow volumes

Watershed	Estimated volume of mobilized material in debris flow (m ³)
W2	1.4E+05
W3	4.5E+05
W4	7.4E+04
W10	1.8E+05

**Figure 16** Tanzania landslide susceptibility map (Kilimanjaro region with high susceptibility marked in red)

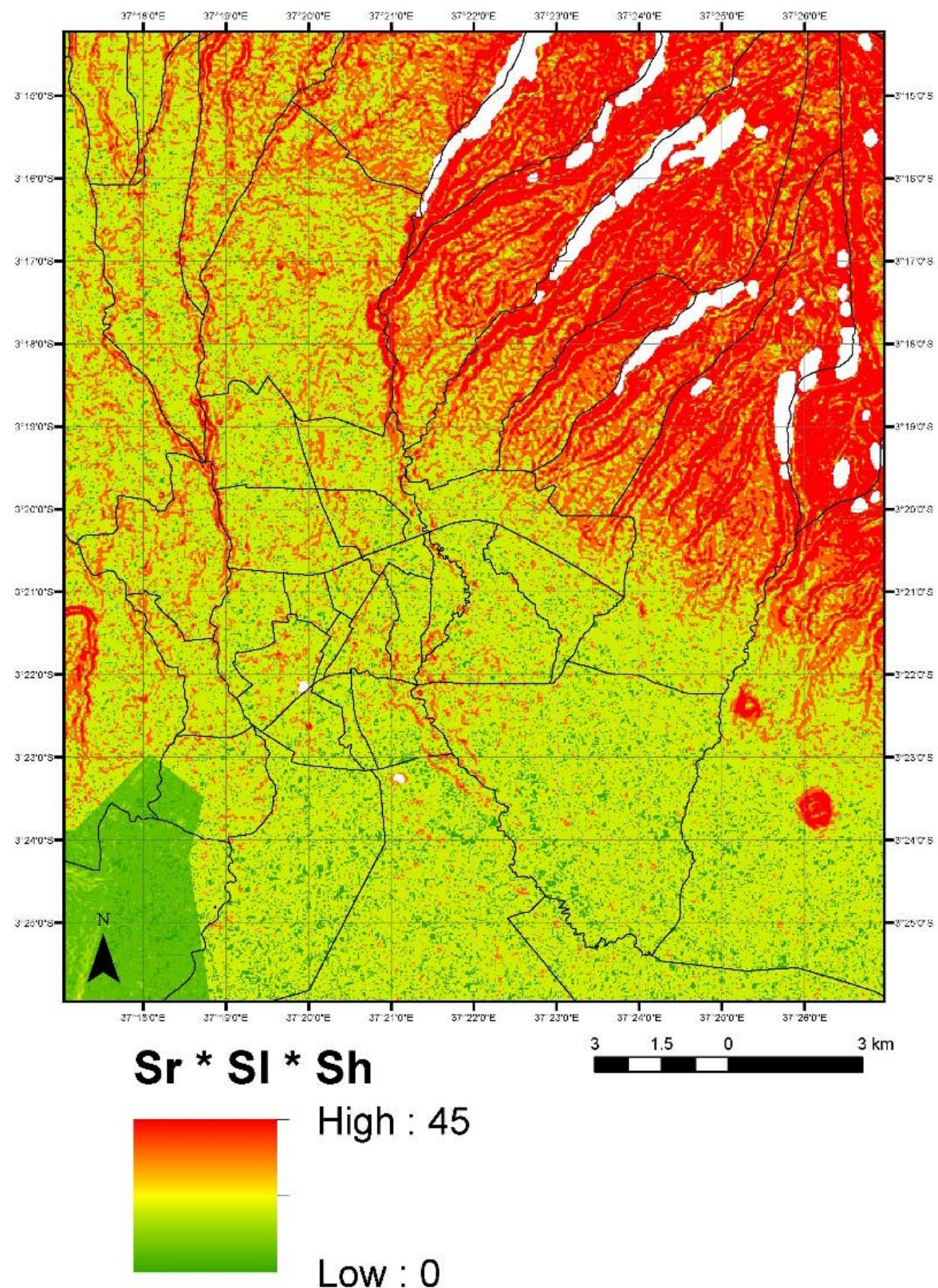


Figure 17 Landslide susceptibility north of Moshi.

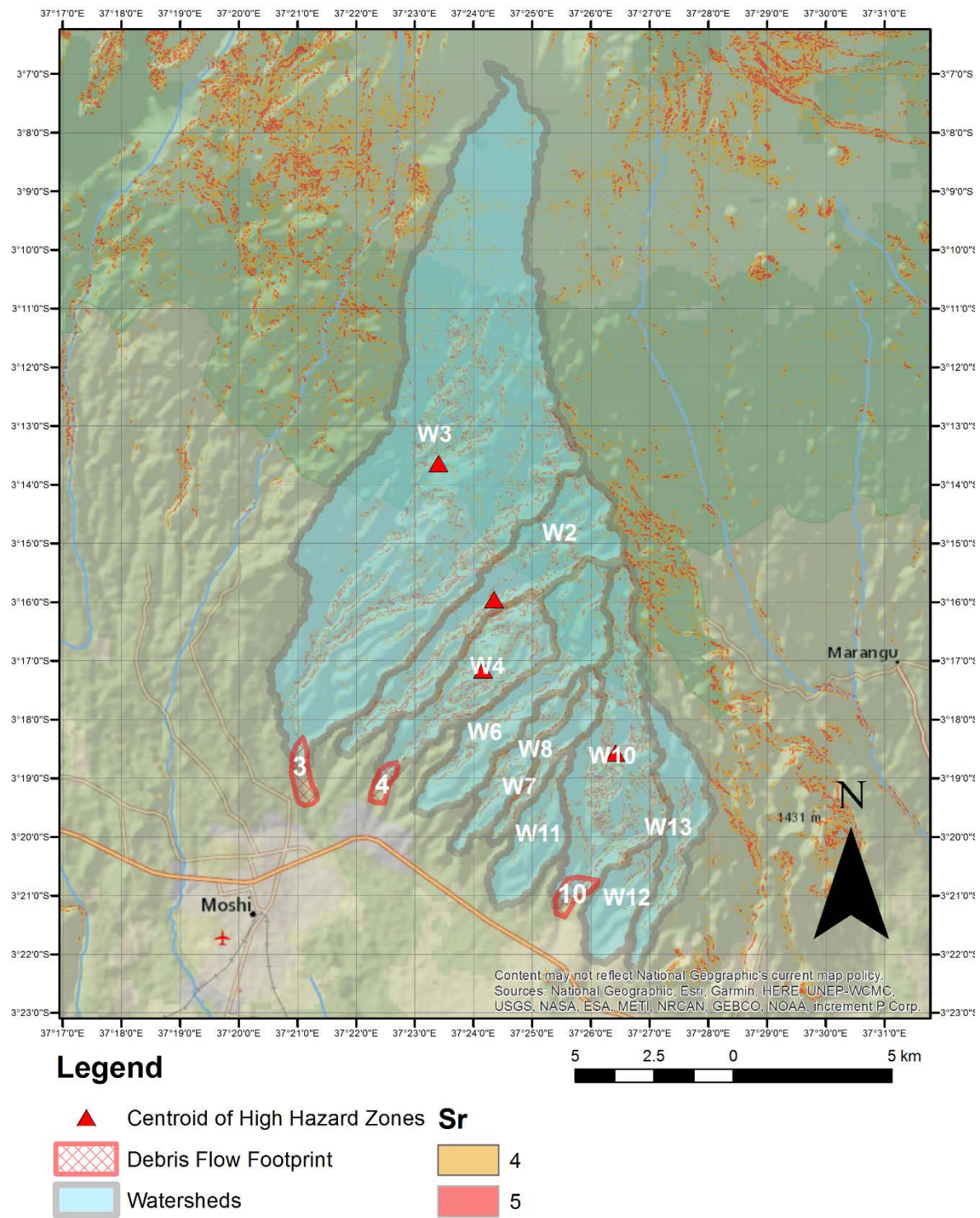


Figure 18 Watersheds northeast of Moshi.

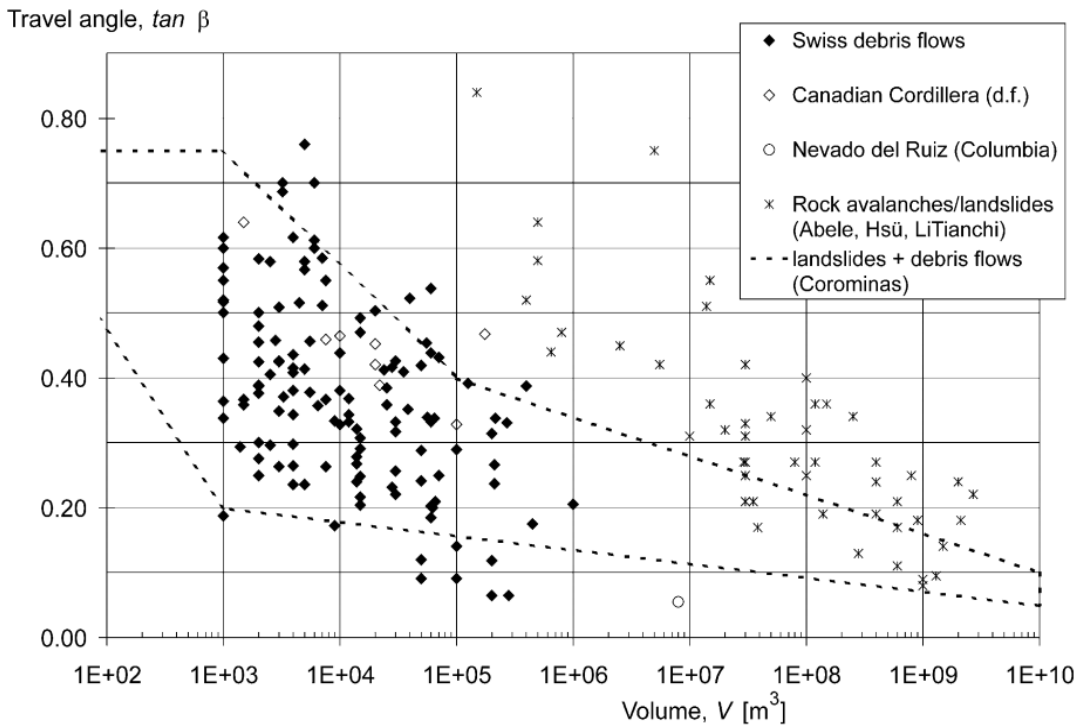
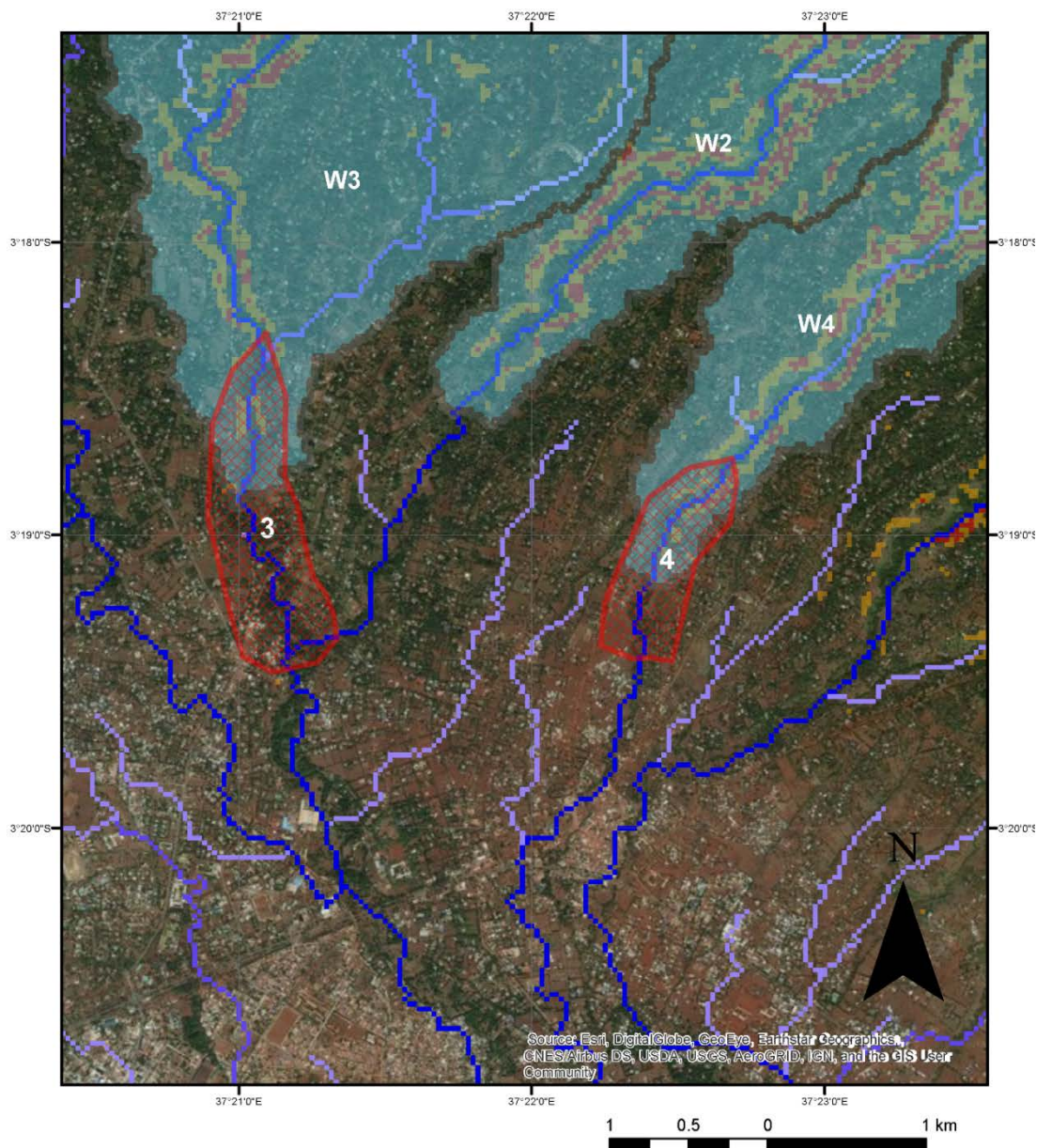


Figure 19 Figure by Rickenmann (2005) showing relationships between the ratio of decrease in elevation to runout distance ($\tan \beta$) and the volume of mass movement. The dashed line shows the approximate boundary that bounds the Swiss debris flow events compiled by Corominas (1996).

5.3 SUMMARY

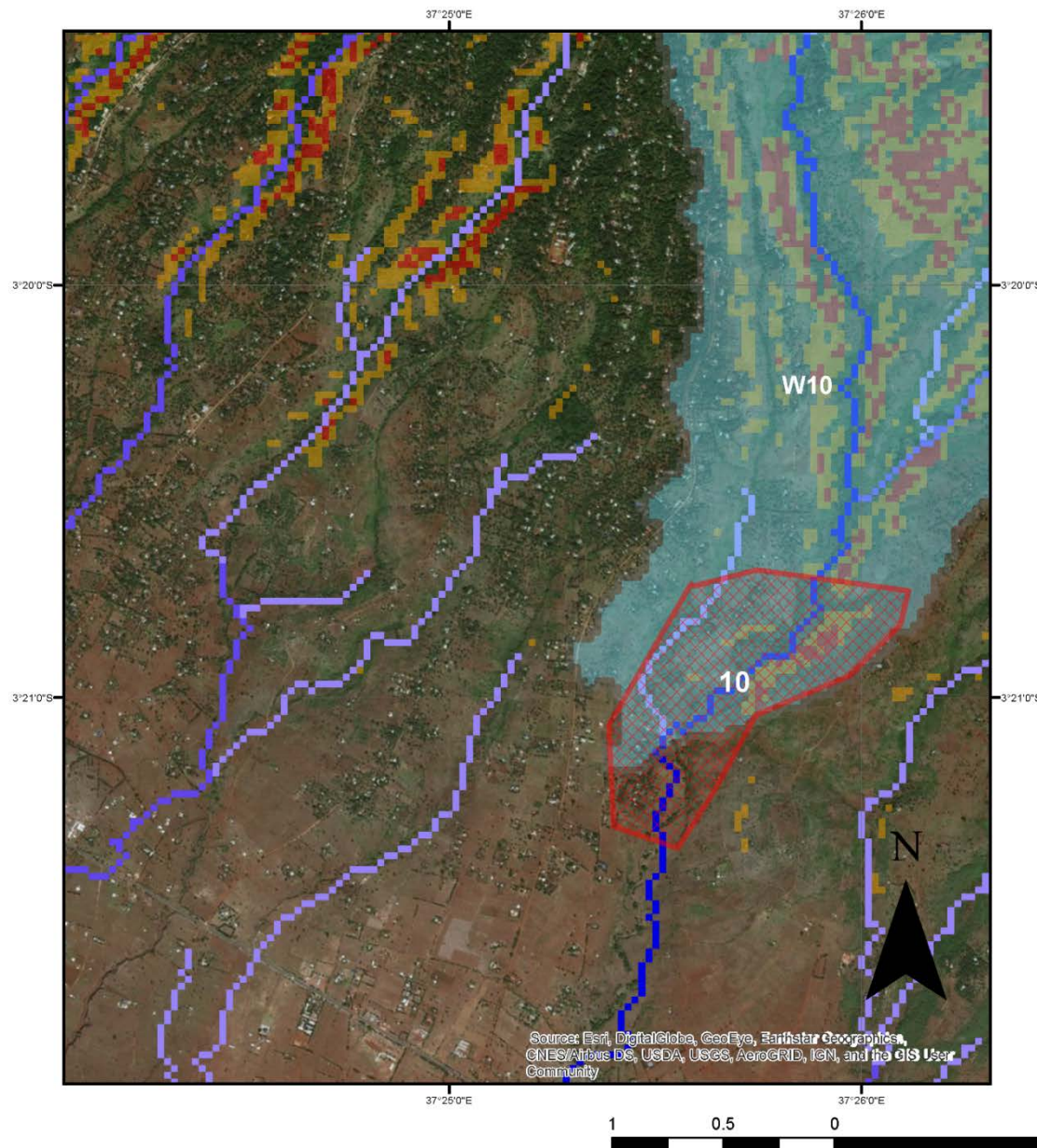
Landslides due to heavy precipitation are analysed in terms of susceptibility. Seismically-induced landslides were not included at present. The historical catalogue also reveal that landslides in Tanzania are predominantly triggered by heavy rain. Soil moisture, lithology, and slope is taken into account in the susceptibility model. Return periods are not assessed, but events represent credible worst case scenarios, which are likely to be significantly more frequent than the tsunami scenarios analysed. Two critical landslide areas are identified, one in the North East close to Kilimajaro, and one in the Southwestern part of Tanzania. Due to the large scenario landslide volumes, buildings impacted by the present landslide scenarios are likely to be fully destroyed. The areas of the highest landslide hazard also represent the areas where landslides have been most frequent historically. *Due to the higher frequency of landslides and the population density in the identified susceptible areas, the landslide risk is considerable.*



Legend

	Centroid of High Hazard Zones	Drainage Network	Sr
	Debris Flow Footprint	Drained Area (no. raster cells)	4
	Watersheds	0 - 500	5
		500.0000001 - 3 000	
		3 000.0000001 - 10 000	
		10 000.0000001 - 4 539 591	

Figure 20 Sketch of landslide affected zones north Moshi, Kilimanjaro region



Legend

▲ Centroid of High Hazard Zones	Drainage Network	Sr
Debris Flow Footprint	Drained Area (no. raster cells)	4
Watersheds	0 - 500	5
	500.0000001 - 3 000	
	3 000.000001 - 10 000	
	10 000.00001 - 4 539 591	

Figure 21: Sketch of landslide affected zones east of Moshi, Kilimanjaro region

6 Tsunami hazard scenarios⁵

6.1 INTRODUCTION

The earthquake induced tsunami scenarios represent events with approximately 500 years (three scenarios) and 2500 years (three scenarios) inundation height return periods. The estimated coastal inundation for these scenarios ranges from about 30 cm representing the mean value for the smallest scenarios, up to about 5 m, representing the maximum inundation values for the largest scenarios. Tsunami travel times are several hours, which should, in principle, make it possible to warn the coastal population. It is noted that one of the scenarios, the M_w 9.3 Andaman-Sumatra scenario, is close to the 2004 Indian Ocean tsunami in strength. *Altogether, the combination of moderate inundation heights, possible tsunami warning, and long return periods, render the tsunami risk towards Tanzania low.*

6.2 TSUNAMI HAZARD METHODOLOGY AND RESULTS

This section briefly describes the methodology for creating tsunami scenarios and their footprints along the coastline of Tanzania. Only far-field earthquake sources are considered. The far-field earthquake sources represent scenarios originating from three different subduction zones, namely Sumatra-Andaman, Sumatra, and Makran. They all represent tsunami events with high return periods, typically a few hundred years and larger. The methodology for deriving the scenarios is outlined below.

The scenarios are derived based on hazard levels from probabilistic tsunami hazard study (Davies et al., 2017) based on the tsunami study for the Global Assessment Report, GAR15 (Løvholt et al., 2015a). The scenarios are extracted based on the post GAR15 hazard levels (Davies et al., 2017) for Tanzania for roughly 500 years (smallest scenarios) and 2500 years (largest scenarios) return periods. From the post-hazard study, hazard levels along the coastline of Tanzania (median inundation heights) of roughly 0.5 m and 0.8 m were determined. Then, the scenarios with earthquake moment magnitudes and locations providing tsunami inundation closest to these respective thresholds were derived for each of the three subduction zones.

Table 10 Earthquake scenario fault parameters

	andmw8.6	andmw9.3	summw8.8	summw9.5	makmw8.7	makmw9.3
Moment magnitude	8.6	9.3	8.8	9.5	8.7	9.3
Mean fault length [km]	282	1095*	363	882	318	679
Mean fault width [km]	102	170	126	260	114	211
Mean fault slip [m]	11.6	17*	14.6	24.4	13	19.4
Dip angle [degrees]	15	15	15	15	15	15
Fault rigidity [GPa]	30	30	30	30	30	30

*Segmented fault.

⁵ Finn Løvholt, Craig Christenson, Bjørn Kalsnes, reviewed by Farrokh Nadim, Norwegian Geotechnical Institution.

Then, deterministic tsunami scenarios were derived. For each scenario, earthquake-induced seabed displacements were computed using an elastic halfspace model (Okada, 1985), assuming uniform pure dip-slip over the fault. An earthquake scaling law (Blaser et al., 2010) was used to derive scenario mean fault length, width, and slip. The fault rigidity was fixed to 30 GPa. Scenario fault parameters are listed in Table 10. A low pass filter removing high frequency components was applied thereafter to convey the seabed slip values to the initial water surface elevations, used as initial conditions for the tsunami simulation (Løvholt et al., 2015b). The initial surface elevations for each scenario were then used as initial conditions in a tsunami simulation model (Globouss, Løvholt et al., 2008) for computing the tsunami propagation over the open ocean. ETOPO Bathymetry data and a grid resolution of 1'×1' were employed in the simulations. Simulation results were then extracted at near-shore control points, and median coastal inundation heights were derived using a set of so-called amplification factors (Løvholt et al., 2012), that relate the offshore tsunami height to median coastal inundation heights. The inundation height distribution along shore is then smoothed using a median filter, to remove artificial fluctuations in the hazard level.

The resulting tsunami heights are in the same range as the hazard levels revealed from the post-GAR15 assessment (Davies et al., 2017), although some deviations may occur. The results are displayed both as oceanic maximum tsunami heights and as inundation heights (see Figure 22 to Figure 27). Inundation heights can range from a few decimetres and up to 4-5 metres. The scenarios originating from the Sumatra and Sumatran-Andaman subduction zones tended to give somewhat larger results than Davies et al., (2017), whereas the Makran scenarios gave slightly lower hazard levels. Generally, the earthquake potential in the Sumatra and Sumatra-Andaman subduction zones is considered much larger than for Makran, and hence, the scenarios along these two subduction zones are considered more probable to occur than corresponding events originating from the Makran Trench. Sumatra and Sumatra-Andaman earthquakes therefore contribute more strongly to the tsunami hazard level in Tanzania. Moreover, the largest Sumatra-Andaman scenario represents a scenario with similar strength as the 2004 Indian Ocean tsunami. We also note that the scenario footprints fully encompass the coastline of Tanzania as well as certain parts of neighbouring country coastlines. Finally, it is noted that tsunami travel times for the Makran scenarios range from 6 to 7 hours, whereas at least 8-9 hours travel times are expected for the Sumatra and Sumatra-Andaman scenarios.

The impact metrics presented here represent both the mean tsunami inundation height and the 90 percentile. The first quantity represents a typical value of the inundation height at any given position at the shoreline. However, the inundation height can vary significantly depending on the position along the coast, and it is not unusual that the maximum inundation height at a location can be 2 to 3 times larger than the mean height. Hence, the estimated local inundation height has considerable uncertainty. The 90 percentile represents the upper range of the statistical distribution of tsunami inundation height using a lognormal distribution and is considered a more representative quantity for the maximum inundation than the mean tsunami inundation. For example, the largest 90 percentile heights for the M_w 9.3 Andaman-Sumatra scenario (3-4 m, see Figure 23 lower right) corresponds closely with the largest maximum inundation heights observed for Tanzania following the 2004 Indian Ocean event (3.5 m). As displayed in Figure 23, Figure 25 and Figure 27, the 90 percentile inundation height is considerably larger than the mean inundation height. This uncertainty is reflected in the uncertainty parameter reported for the scenarios below. It is therefore stressed that the present hazard levels *should not be used for local studies*. For this

purpose, for instance towards sites with large coastal population, refined studies need to be carried out. The present hazard maps gives an indication of possible hazard levels from far-field tsunamis, which can be used for more detailed planning and comparison with other hazards. More refined studies can use the present scenarios as input conditions, but would need high resolution coastal topography data as input, and availability of local tsunami inundation models (e.g. Kanoglu et al., 2015).

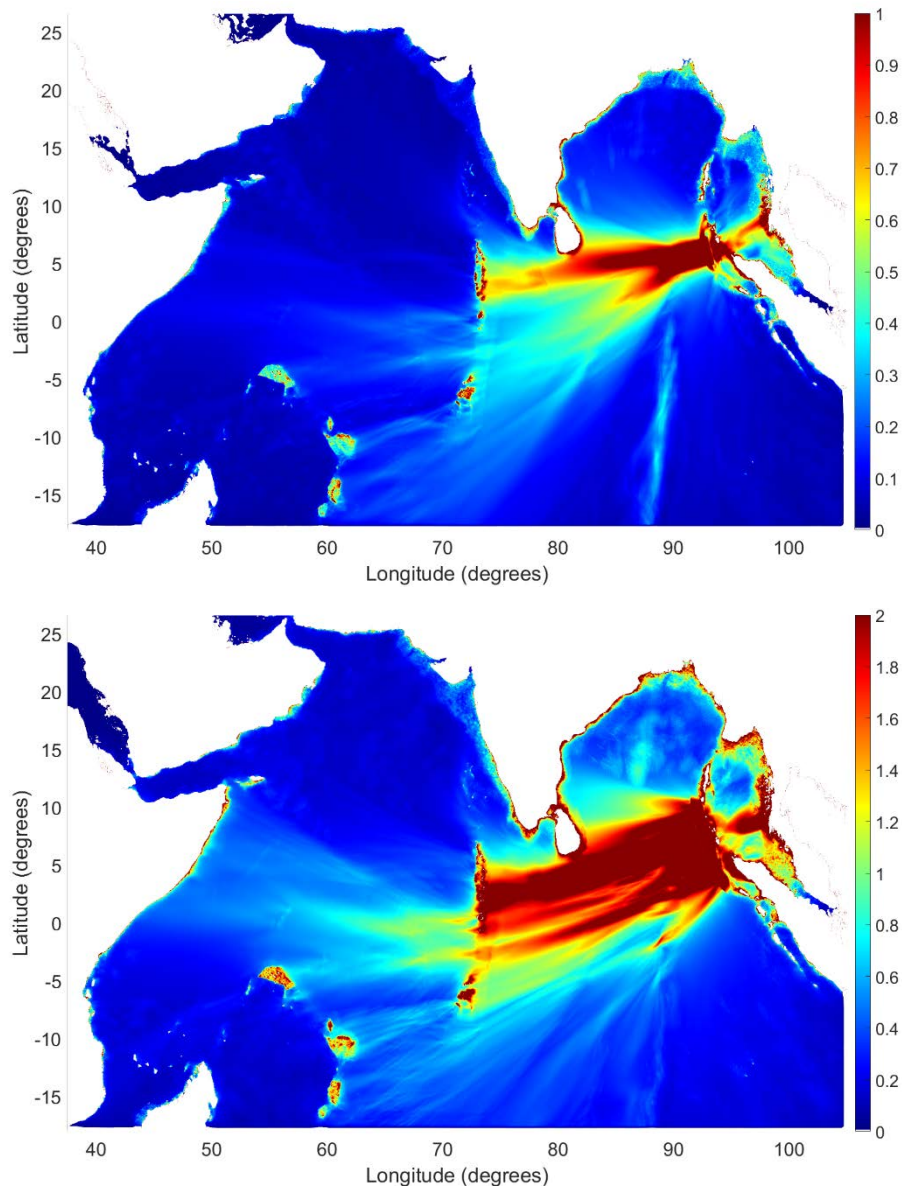


Figure 22 Sumatra-Andaman Trench scenarios, maximum surface elevation. Upper Mw8.6 scenario, lower Mw9.3 scenario.

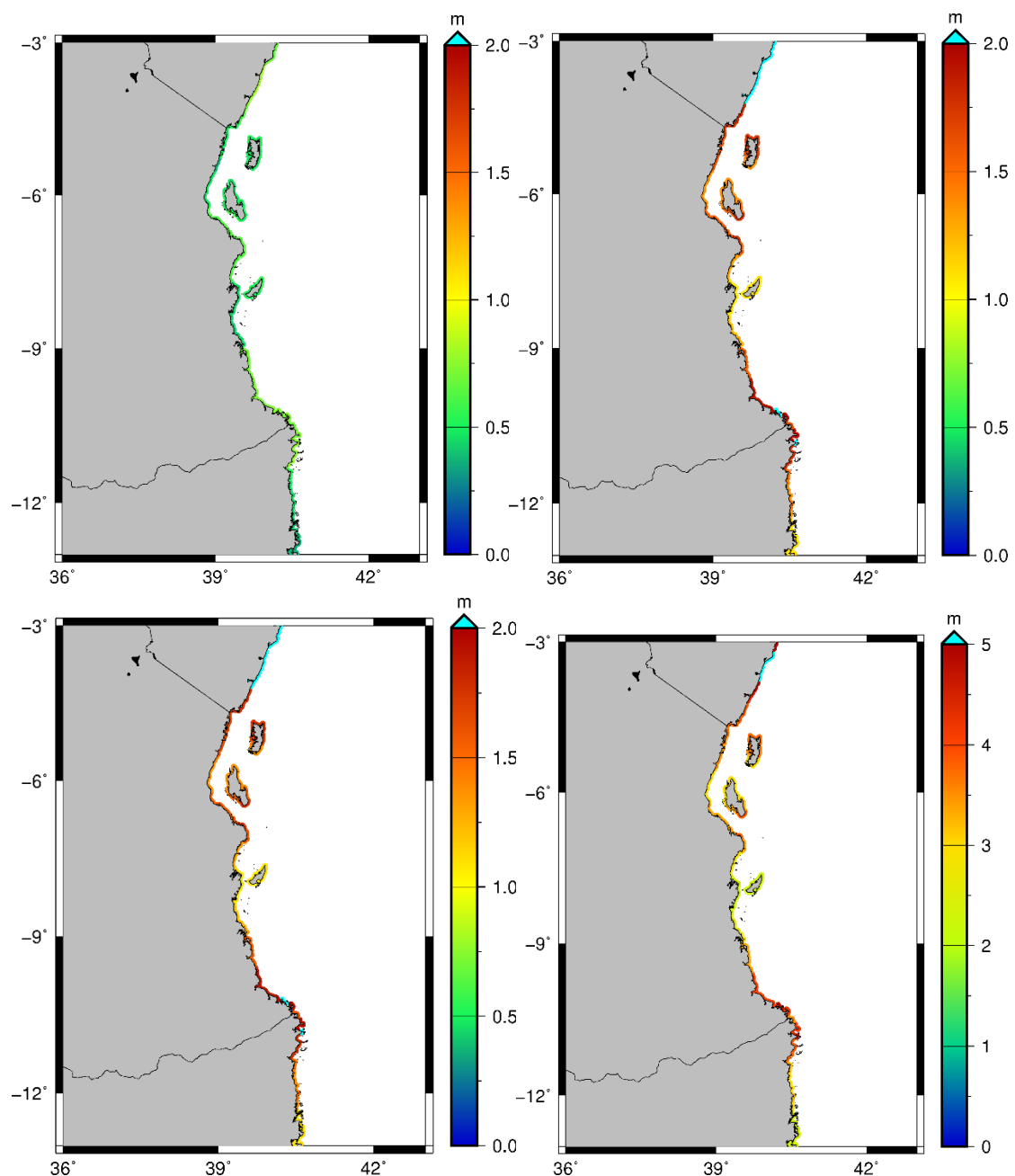


Figure 23 Coastal inundation heights for Sumatra-Andaman Trench scenarios. Upper panels M_w8.6 scenario, lower panels M_w9.3 scenario. Left panels, mean values. Right panels, 90 percentile inundation heights.

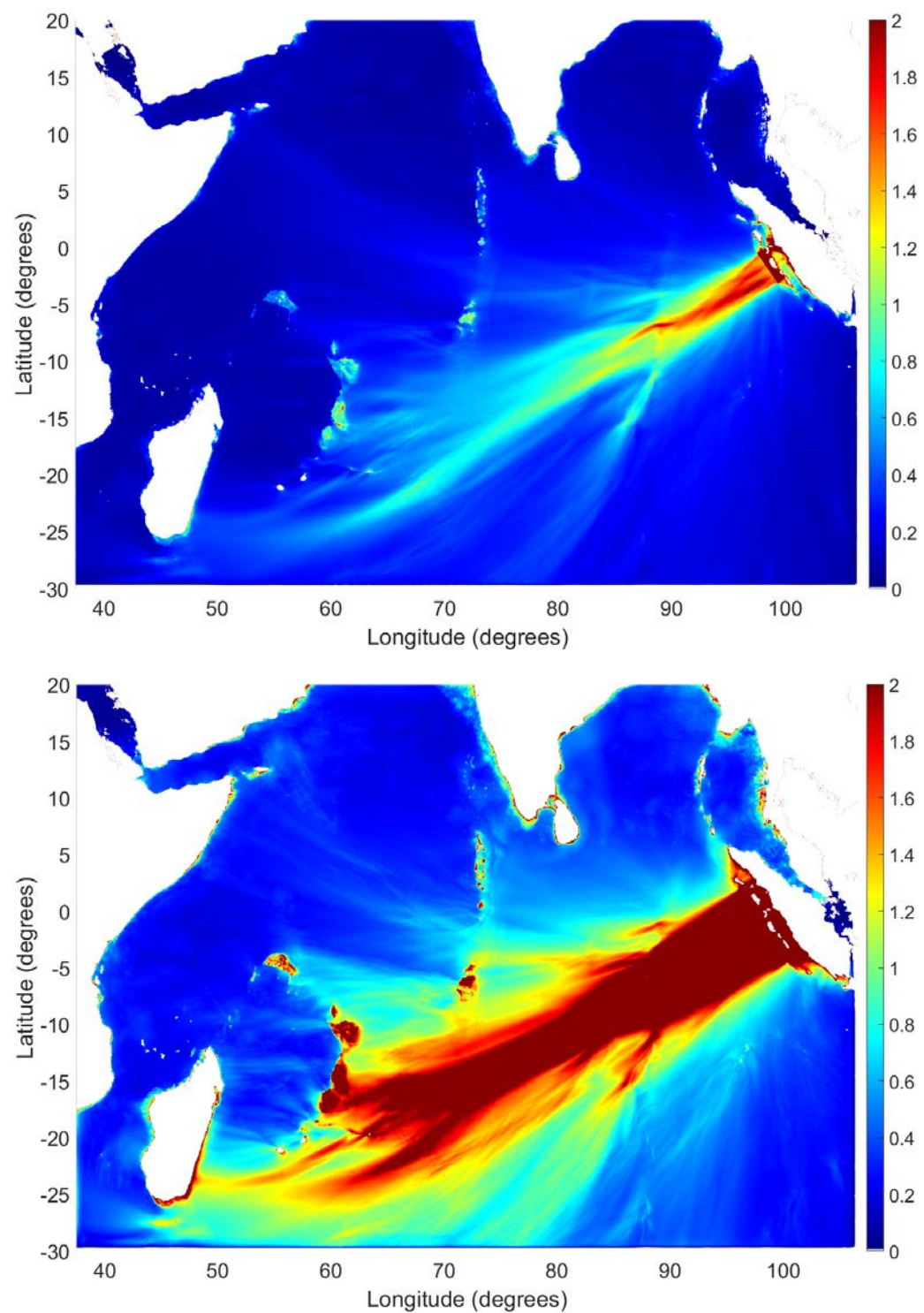


Figure 24 Sumatra Trench scenarios, maximum surface elevation. Upper $M_w 8.8$ scenario, lower $M_w 9.5$ scenario.

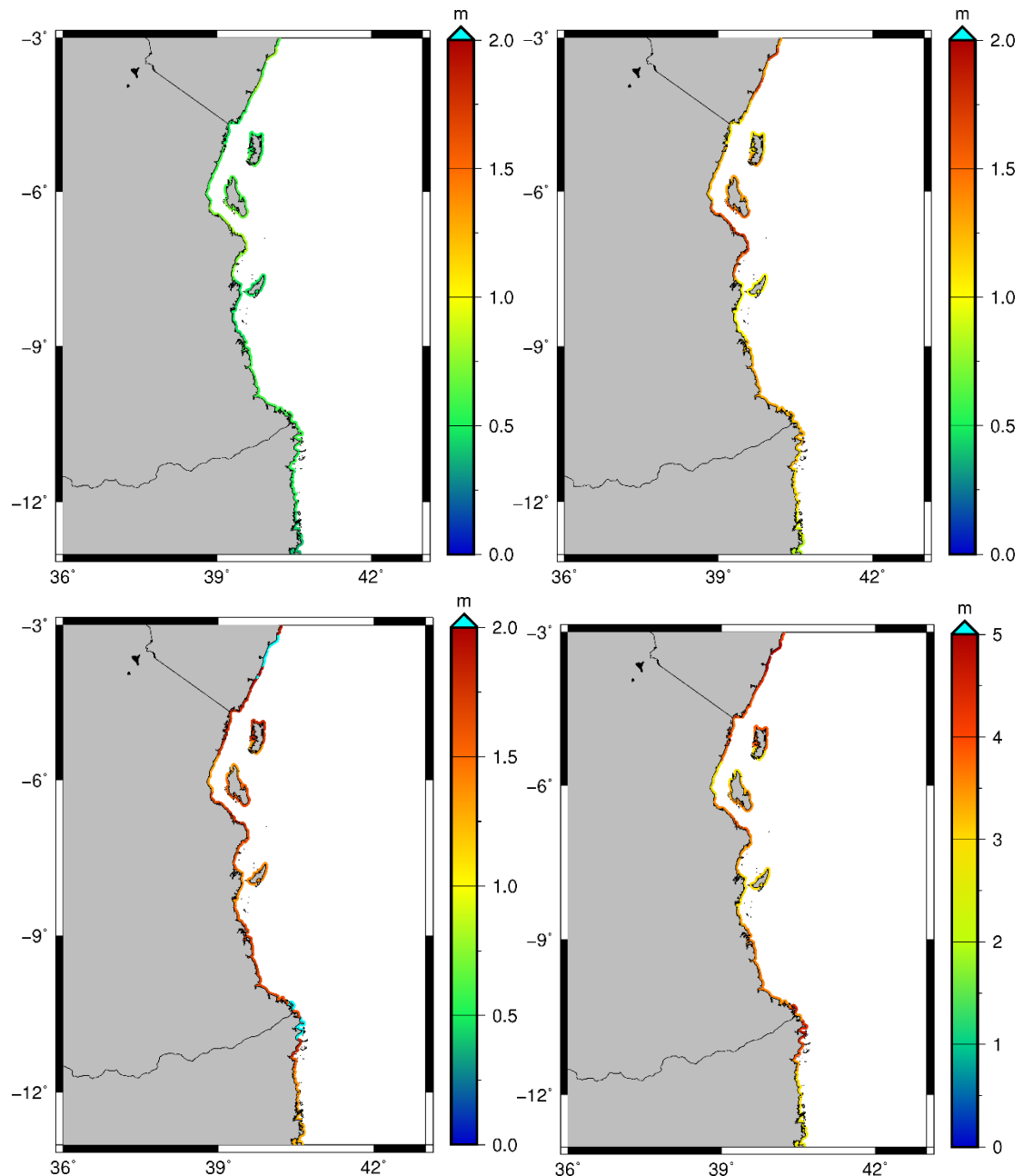


Figure 25 Coastal inundation heights for the Sumatra Trench scenarios. Upper panels $M_w 8.8$ scenario, lower panels $M_w 9.5$ scenario. Left panels, mean values. Right panels, 90 percentile inundation heights.

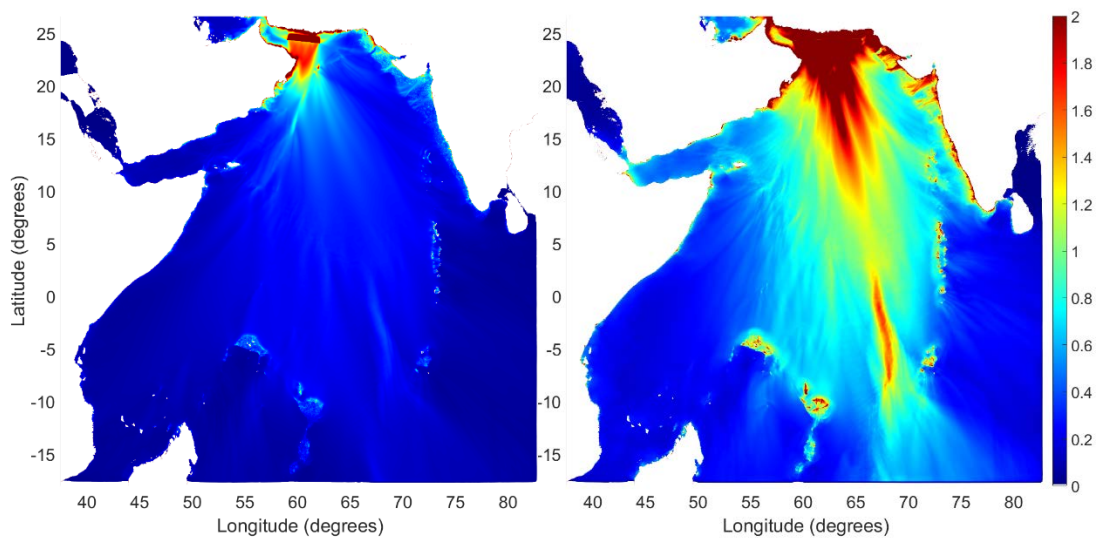


Figure 26 Makran Trench scenarios, maximum surface elevation. Left $M_w 8.7$ scenario, right $M_w 9.3$ scenario.

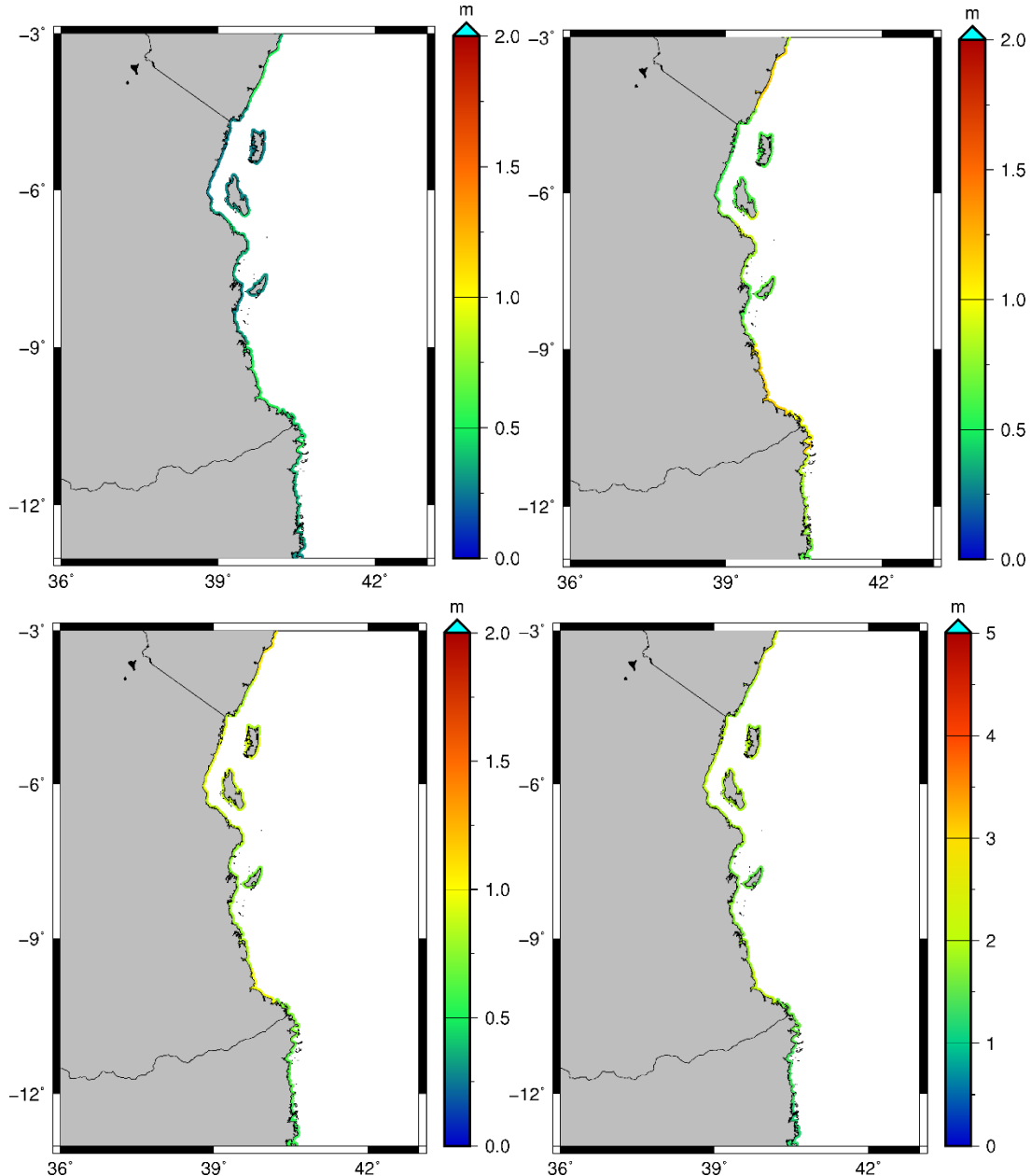


Figure 27 Coastal inundation heights for the Sumatra Trench scenarios. Upper panels $M_w8.8$ scenario, lower panels $M_w9.5$ scenario. Left panels, mean values. Right panels, 90 percentile inundation heights.

6.3 SUMMARY

These tsunami scenarios represent events with relatively low probability / high consequences and approximately 500-2500 years inundation height return periods. The estimated coastal inundation for these scenarios range from about 30 cm representing the mean value and the smallest scenarios, up to about 5 m inundation height, representing the expected maximum inundation for the largest scenarios. Tsunami travel times are several hours, which should in principle make it possible to warn the coastal population. It is noted that one of the scenarios, the M_w 9.3 Andaman-Sumatra scenario, is close to the 2004 Indian Ocean tsunami in strength. None of the scenarios provide larger waves than this scenario, which means that stronger events should be associated with even longer return periods. However, as shown in this report, several other source zones can provide a

similar threat. The tsunami analysis is coarse grained, and to quantify the coastal hazard more specifically, local analysis should be carried out. Altogether, the combination of moderate inundation heights, possible tsunami warning, and long return periods, makes the tsunami risk towards Tanzania low.

Tsunami hazard data use: The tsunami analysis is coarse grained, and can be used for identifying typical values for tsunami hazard metric. In order to link the scenario tsunami hazard used to vulnerability functions, inundation maps quantifying the flow depth over land is needed. However, the hazard values are only available at the shoreline points, meaning that the extent of horizontal inundation and the flow depth is not quantified. Therefore, to quantify the coastal hazard more accurately, and to provide a link to vulnerability and exposure, additional local analysis needs to be carried out. The tsunami hazard data are uncertain, associated with a lognormal uncertainty distribution. From this distribution, the mean values represent typical inundation heights, whereas the 90 percentile values given within the represent values that would typically represent the maximum inundation height along the coastline. It is important also to note that the return periods for each scenario hazard is representative for the aggregate exceedance probability of the coastal inundation height posed by all earthquake sources (all the individual scenarios therefore have different probability).

Tsunami hazard, possible short term improvements: Deriving scenarios for more return periods, for instance smaller scenarios is relatively straightforward. However, without high resolution Digital Elevation Models (DEM's) (e.g. using globally available SRTM data), inundation will often be artificially low, and it is therefore only advisable to do inundation mapping based on high resolution topography. If local high resolution DEMs for the topography are made available for a location of interest, more accurate (less uncertain) local inundation hazard maps can be simulated and uploaded to the data schema. With high resolution DEM's, the present shoreline hazard data can also be extrapolated to roughly quantify inundation extent, although this is less accurate than performing local simulations (more uncertain).

7 Flooding hazard scenarios⁶

7.1 INTRODUCTION

In the case of floods, a hazard map for 100 years return period was calculated in terms of water depths and an event set of 20 scenarios that were selected with various severities was delivered. The hazard intensity is the expected value of water depths and uncertainty is given in terms of standard deviation of such water depth in each scenario event.

7.2 METHODOLOGY

The conceptual modelling framework is shown in Figure 28. The methodology is adopted from the approach used for GAR 15, the Global Flood Model (Rudari et al. 2015). The various datasets used for the global modelling are described in Rudari et al. 2015 and include: river discharge datasets, reservoir and dam database, Digital Elevation Model and hydrological derived datasets, land cover datasets, climatic datasets, recorded flood event dataset.

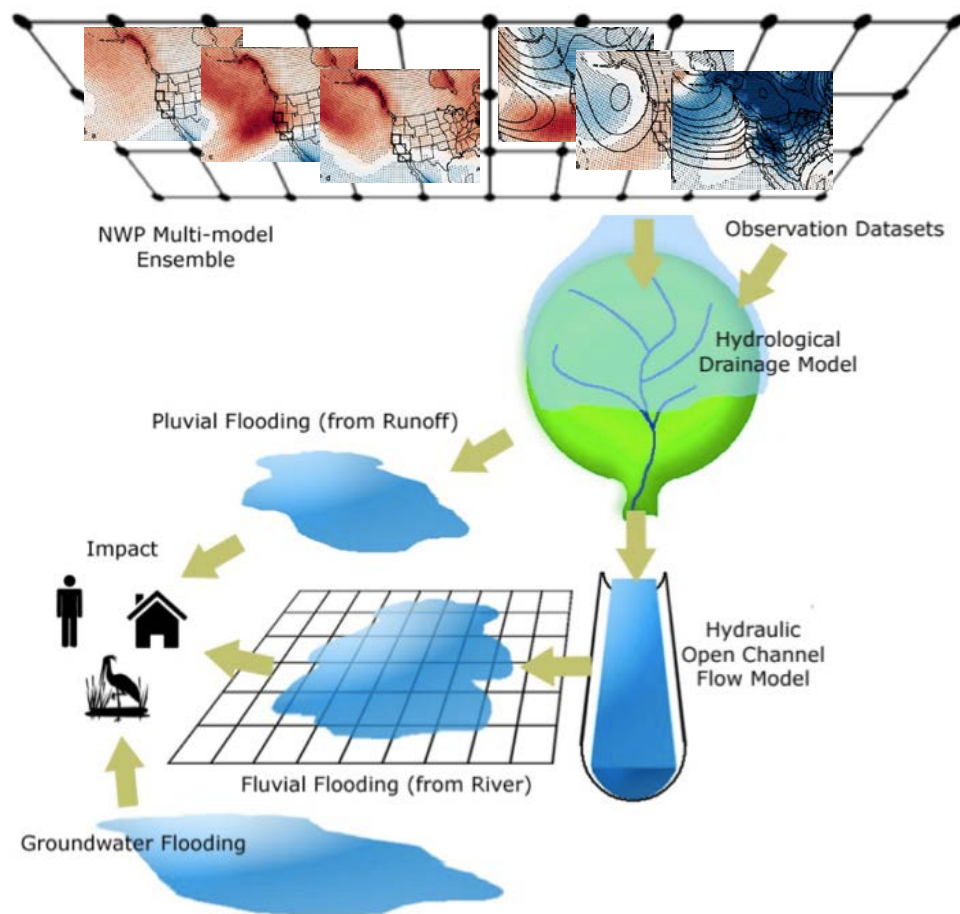


Figure 28 The conceptual modelling framework used for flood hazard scenarios.

⁶ R. Rudari, CIMA

A full dynamic weather generator has been used to generate a first set of flood scenarios with associated uncertainty. As a second step, these scenarios have been expanded using statistical techniques to match the scenarios set exhaustivity.

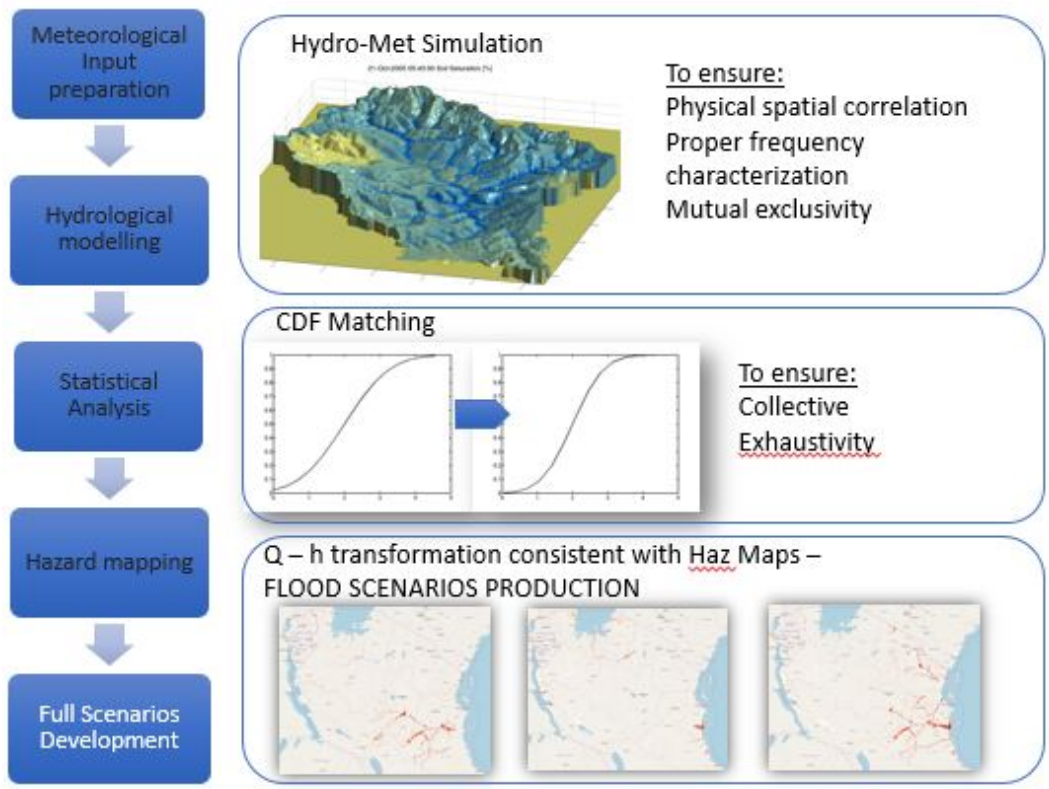


Figure 29 Schematic showing full computation of the scenarios.

7.3 RESULTS

The event set is for the whole of Tanzania and has generated scenarios for one of the largest floods country-wide, one of the largest simulated floods in the coastal regions and one of the largest simulated floods in southern Tanzania (Figure 30). See Annex for the full scenario metadata.

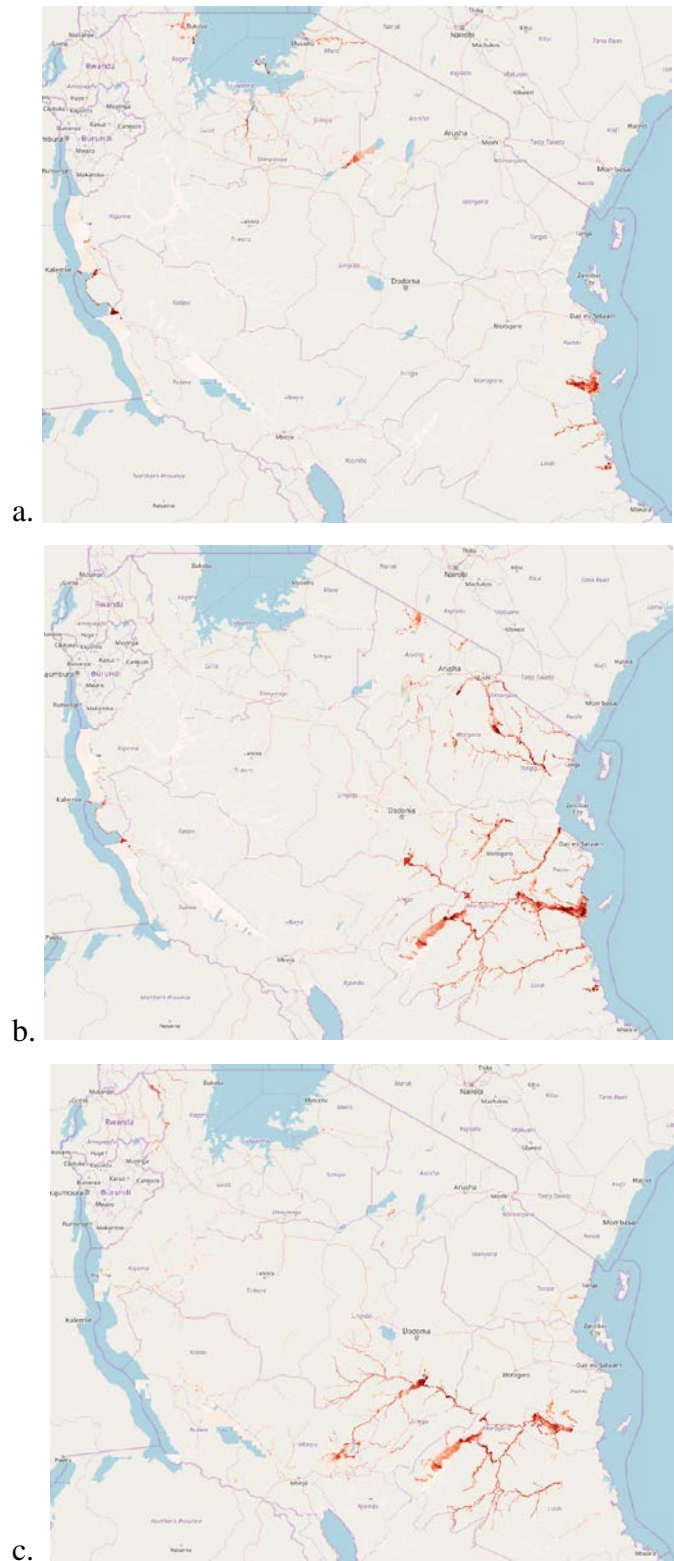


Figure 30 a. One of the largest simulated events in the coastal zone of Tanzania. b. One of the largest simulated events country-wide in Tanzania. c. One of the largest simulated events in southern Tanzania.

8 Drought hazard scenarios⁷

Droughts as a natural hazard are complex to assess and not as straightforward to compare with hazards such as floods or earthquakes. This has to do with the fact that droughts build up over time and lack a distinct trigger as is the case with many other hazards. Moreover, identification of drought conditions is constrained in both time and space as water resources can be transferred through space (i.e. coming from upstream) and time (i.e. impact of a dry month depends also on the conditions of previous months). Lastly, drought conditions are often relative, as humans and environment have adapted to conditions in a certain place. As a result of all these complexities, a lot of indicators have been developed for droughts, and various types of droughts are usually determined in the literature (i.e. meteorological, hydrological, agricultural and socio-economic droughts). It is therefore important to explore a range of indicators for droughts and determine which ones are most applicable for a certain situation/location. Therefore, we developed scenarios for five indicators of drought hazard and compiled a database of historical drought events to compare these with. Given that a transportable methodology is wanted, globally available data has been used for this.

8.1 HISTORICAL DROUGHTS

We consulted two major databases on drought events (EM-DAT and the Munich Re NatCat database) on drought events for the target country of Tanzania. Next to these two databases, we also consulted various other sources of literature to determine when drought events happened in Tanzania. This resulted in three time lines of drought events in Tanzania, which did not everywhere agree. On four occasions all three sources agreed on the presence of drought conditions: 1984, 1991-1992, 1998-1999, and 2006 (Figure 28)

⁷ Developed by: Tristian Stolte, Ted Veldkamp and Hans de Moel from the Vrije Universiteit Amsterdam

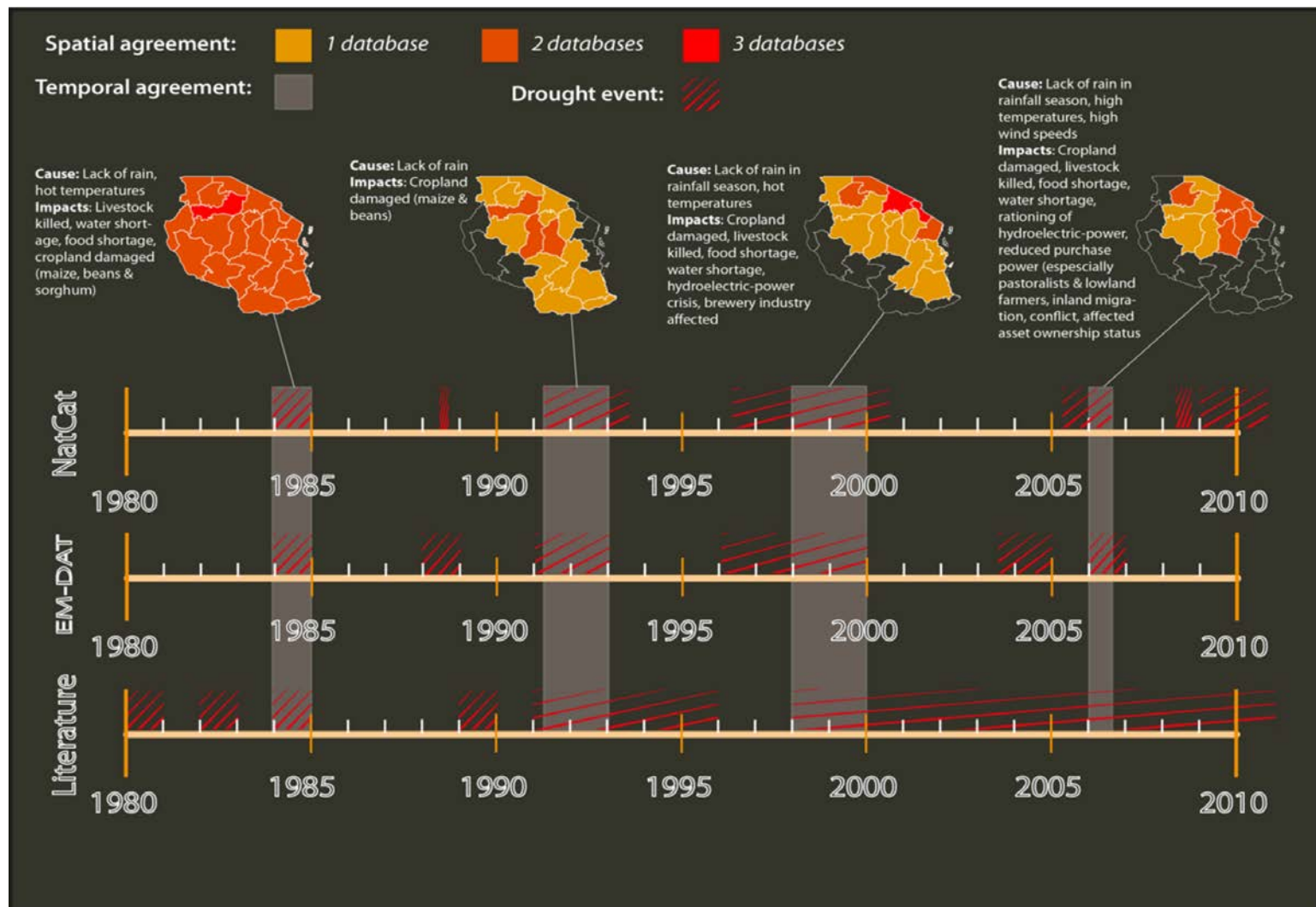


Figure 31 Comparison of drought events according to three databases, including their spatial extent according to the sources

8.2 INDICATORS

In order to be applicable in any region, use has been made of globally available information. This consists mainly of input and results of the WaterGAP3 hydrological model using data from 1983-2012 (available through ISIMIP) which calculates hydrological variables at the global scale on a 0.5 degrees grid. Runs that were forced with the Era-Interim adjusted Watch Forcing Data (known as WFDEI) have been used for this study. With this data, five indicators have been calculated:

- **Standardized Precipitation Index (SPI):** which denotes the accumulated precipitation (per month) with respect to the long-term average precipitation (of that month). This results in a standardized score with a mean of 0 and a standard deviation of 1.
- **Standardized Precipitation-Evaporation Index (SPEI):** similar to the SPI, but instead of just taking precipitation, the net precipitation is taken by subtracting the evaporation before standardizing it.
- **Standardized Runoff Index (SRI):** denotes the runoff in a grid-cell, which includes not only precipitation and evaporation, but also interaction with various reservoirs such as the soil and groundwater. This is basically the result of the water balance in a given grid cell, without any influence from upstream cells. Like SP(E)I this is standardized to reflect the deviation of the long term average runoff in the grid cell.
- **Standardized Stream Flow Index (SSFI):** similar to SRI, but now including the input from upstream grid cells. This concerns thus the streamflow or discharge as one could measure in a river or stream. Standardized in a similar way as the other indices.
- **Standardized Soil Moisture Index (SSMI):** this concerns the water present in the soil reservoir, which has again been standardized using the long term average to scores with a mean of 0 and a standard deviation of 1.

Each of the above indicators has been calculated for every month in the time series. As they all have a mean of 0, and a standard deviation of 1 they can be compared directly. As droughts are a relative concept, (strong) negative values denote dry conditions. Here we use a threshold of -1 to denote dry conditions (i.e. values < -1 add to a drought). As dry conditions can last over several months (or even years) we accumulate deficits over time. If a month has a value lower than -1, the difference is added to the deficit (i.e. a month with a value of -3 adds 2 to the deficit). This adds up over time and for each year the largest deficit can be determined. A high score thus denotes that dry conditions were long and/or strong. With scores for each year (and each grid cell), return periods of certain scores could be calculated empirically, and subsequently mapped. This has been done for 1/2, 1/4, 1/10, 1/20, 1/50 and 1/60 years (Figure 29). This shows that meteorological drought (as SPEI denotes) increases relatively gradually with return periods, with at very high return periods (1/50 years) particularly affected the central and south-central regions of Tanzania. The streamflow based index (SSFI) denotes a less gradual increase with return periods, indicating that hydrological drought conditions are not so frequent as meteorological drought conditions. From return periods of once in 10 years they start to affect regions, particularly in the northeast and northwest of the Tanzania (Figure 29).

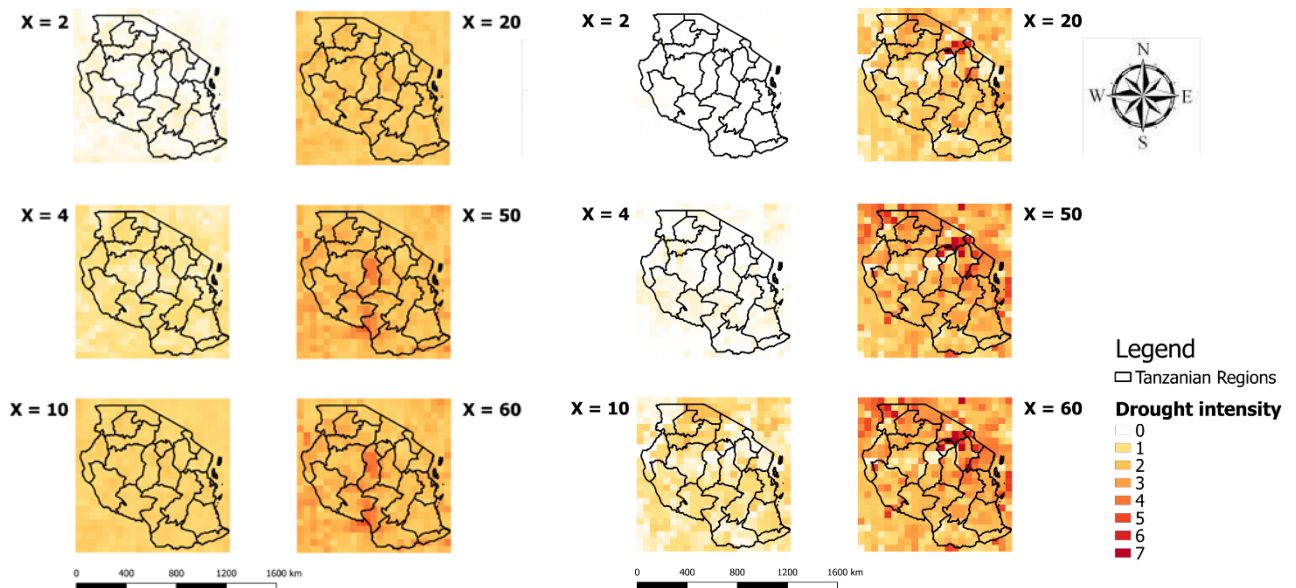


Figure 32 SPEI (left) and SSFI (right) for various return periods (denoted by X).

Next to these parameters, also the overall water availability per capita has been estimated (known as the water crowding index). This is an established indicator for water scarcity and denotes the self-sufficiency of water in a particular region. It is calculated by summing the total available water for a year and dividing this over the total population in a given region. Here we have calculated it at the grid cell level. This denotes in which areas one is reliant on (virtual) water from elsewhere, this could be from streamflow from upstream, or by importing food from other regions (where one basically uses the water resources of another area). The result is strongly population driven, as can be seen in Figure 30, where high water scarcity is found in the Dar es Salaam and the north of Tanzania.

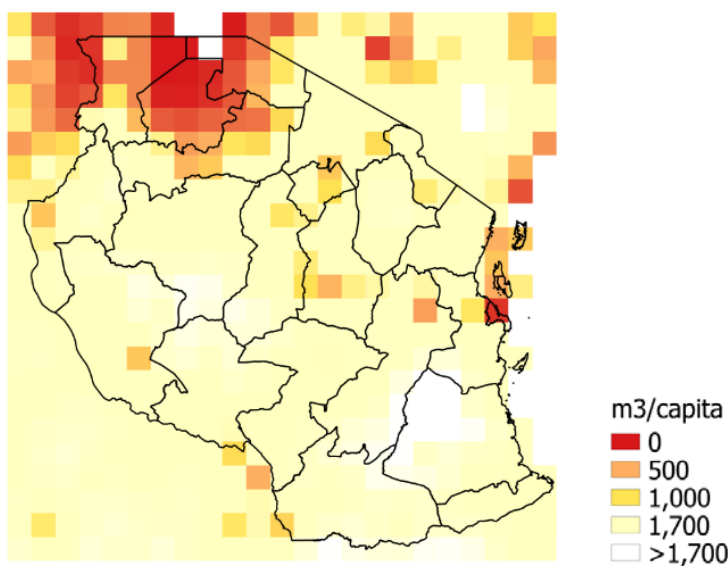


Figure 33 Water crowding index. Values below $500 \text{ m}^3/\text{capita}/\text{year}$ indicate extreme water scarcity.

8.3 COMPARISON

With a historical time-line of droughts established from databases and literature and calculation of a variety of drought indicators, a comparison can be made on how they correspond. Generally, the correspondence is not as high as one would expect or hope. Figure 31 shows the 1984 drought event, which was one of historic proportions. According to the literature and database basically the entire country was affected (see databases map in Figure 31). The indicators actually do not signify particularly dry conditions in the north-east of Tanzania. Mainly the south of Tanzania looks to be affected according to SPI, SPEI and SSMI, whilst SRI and SSFI indicate dry conditions in the south-west. When looking through the entire timeline, 1984 had the lowest SPEI values ever observed at the nation scale, and SPI and SSMI were ranked 3rd lowest at the national scale.

Drought indicator scores during the 1984 drought event for different drought indices

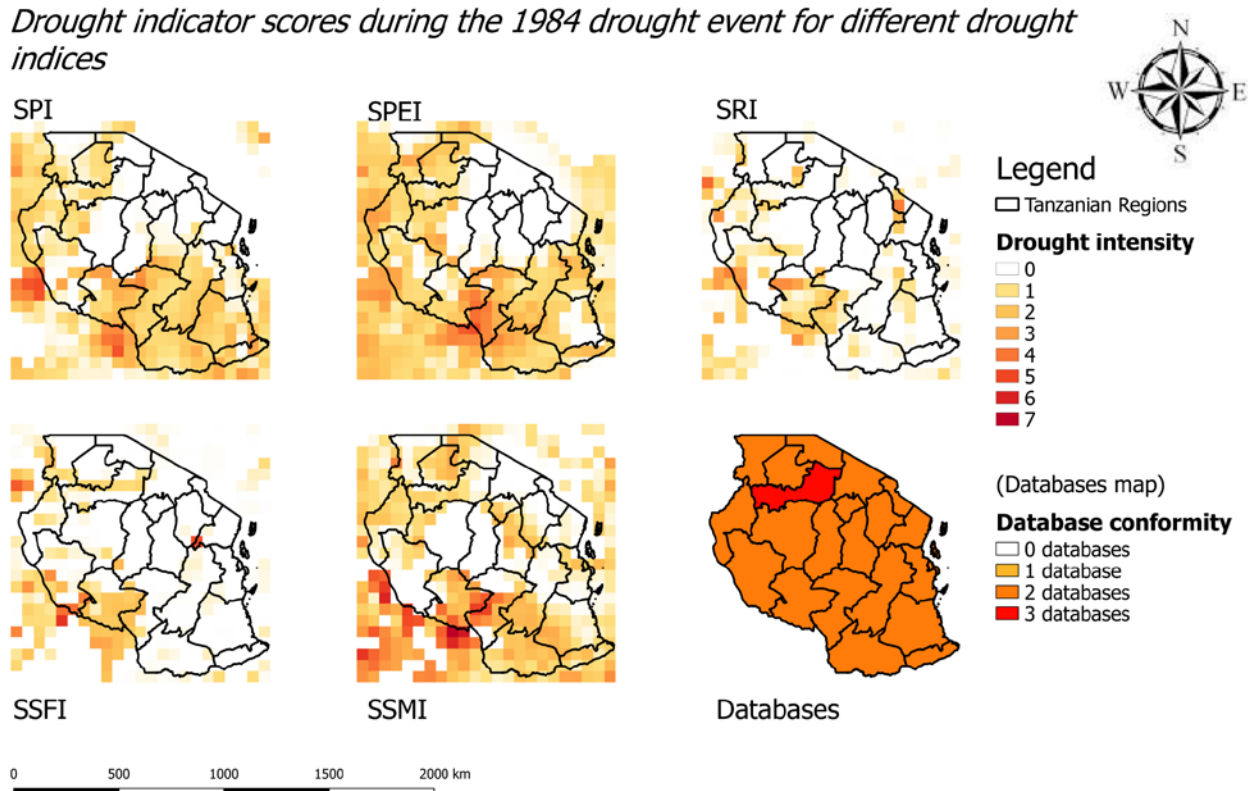


Figure 34 Comparison of drought indicators for the 1984 drought event in Tanzania. Drought intensity is the accumulated deficit (using a threshold of -1).

8.3.1 Guidance on use

It should be kept in mind that different indicators should be used for different things. SPI and SPEI are based on precipitation (and evaporation) and are thus applicable in locations where there is a lot of rainfed agriculture. SSFI on the other hand, is based on water flowing through stream/rivers and thus more applicable in locations where there is irrigation and/or hydropower. Given that most agriculture in Tanzania is rainfed, particularly the SP(E)I indicators should thus be applicable. Indicators such as the water crowding index should be interpreted given the resolution at which they are calculated. Here we calculated them at the grid cell level, which makes it a water self-sufficiency measure, indicating that in areas with a low WCI, population is dependent from water from elsewhere, either from streamflow, or through the import of agricultural products (known as virtual water flows).

8.3.2 Future directions

The relatively poor validation of the calculated indices with observed drought events can be the result of errors/uncertainties on either the database side or the indicator side. The first one is possible to address and should be tackled by cooperation with local scientists from the Tanzanian Met Agency and Ministry of Agriculture to find out which events really impacted Tanzania. From the impact side, the precipitation data used in these calculations could be validated with gauged data to make sure that is in line. However, it is also very possible that the poor comparison results from the fact that drought impacts are likely not only driven by biophysical factors, but may very well be a combination of biophysical factors with social and economic factors. It is anecdotally known that social conflicts and food prices can also play a role in drought events and corresponding famines.

8.3.3 Links with other hazards

Droughts are not directly linked to other hazards in the sense that it can trigger or be triggered by another hazard. However, in terms of build-up it has strong similarities to volcanic hazards where a volcano can be actively erupting for quite a while before exploding (or not). Moreover the impacts of droughts are not necessarily direct losses to assets, but are more related to fatalities, health, well-being and longer term effects in terms of refugees and indirect impacts. In this light, the determination of indirect impacts is particularly important for droughts, and other hazards, volcanic hazards in particular.

9 Overall guidance and use considerations

The hazards proto-database contains scenarios based on existing data for multiple hazards most of which are from global datasets and modelling methodologies carried out for the GAR15. Potential users should be aware that such global datasets and modelling outputs simply highlight areas that are worth investigating further. Local and national hazard assessments should be based on high resolution DEMs (and bathymetry) with data collected for purpose. The current lack of high resolution DEMs and bathymetry is the single biggest barrier to progress in making hazard assessments.

Ideally potential users of hazard data and hazards scientists should have a dialogue to see what areas are of interest and then hazards assessments can be designed to be fit for purpose. Outputs can be iterated depending on user needs. The ability of scientists to meet needs may depend on data availability.

Knowledge gaps should be acknowledged. Catalogues of hazards for Tanzania are not well-established and there is great potential to develop them further using historical records and the stories of those who may have experienced them. Forensic analysis of past events is an excellent means of data collection and can engage communities, authorities and scientists in a common task. Basic data collection is needed from geological and hydrometeorological studies, historical and community records and this creates great opportunities for student projects, training activities and novel research.

The quality of basic data, calibration of data and data management are absolutely crucial in order to start a hazard assessment and create products derived from the data. This project has created the framework necessary to ensure such standards are maintained and documented. There are potential issues around appropriate use of the scenarios. .

It's essential that appropriate information is stored in the data schema relating to reliability, quality assurance, models used, data used. Metadata such as the source of data, the IPR, the purpose for which scenarios have been chosen and modelled need to be captured in the metadata.

Partners in Tanzania have made it very clear that users are unlikely to use scenarios unless they're part of the process that creates them, or the process, purpose and source of the hazards sceanrios is clearly stated.

10 References

- Atkinson G, Boore D (2006) Earthquake ground-motion prediction equations for eastern North America. *Bull Seismol Soc Am* 96:2181–2205
- Brown, S.K., Sparks, R.S.J., Mee, K., Vye-Brown, C., Ilyinskaya, E., Jenkins, S.F. and Loughlin, S.C., 2015. Country and regional profiles of volcanic hazard and risk. In: S.C. Loughlin, R.S.J. Sparks, S.K. Brown, S.F. Jenkins and C. Vye-Brown (Editors), *Global Volcanic Hazards and Risk*. Cambridge University Press, Cambridge, UK, pp. 173. Open Access: cambridge.org/volcano.
- Carey, S. and Sigurdsson, H., 1986. The 1982 eruptions of El Chichon volcano, Mexico (2): Observations and numerical modelling of tephra-fall distribution. *Bulletin of Volcanology*, 48(2-3): 127-141.
- Carey, S. and Sigurdsson, H., 1989. The intensity of plinian eruptions. *Bulletin of Volcanology*, 51(1): 28-40.
- Connor, L.J., Connor, C.B. and Bonadonna, C., 2008. Forecasting tephra dispersion using TEPHRA2. .
- Corominas, J., (1996) The angle of reach as a mobility index for small and large landslides, *Canadian Geotechnical Journal*, Vol. 33, pp. 260-271.
- Dilley, M., Chen, R.S., Deichmann, U., Lerner-Lam, A.L., Arnold, M., et al. (2005): Natural Disaster Hotspots – A Global Risk Analysis. Report, International Bank for Reconstruction and Development/The World Bank and Columbia University: 132.
- De Schutter, A., Kervyn, M., Canters, F., Bosshard-Stadlin, S. A., Songo, M. A. M., Mattson, H. B. 2015. Ash fall impact on vegetation: a remote sensing approach of the Oldoinyo Lengai 2007-08 eruption. *Journal of Applied Volcanology*, 4, 15.
- Fontijn, K., Ernst, G., Bonadonna, C., Elburg, M., Mbede, E. and Jacobs, P., 2011. The ~4-ka Rungwe Pumice (South-Western Tanzania): a wind-still Plinian eruption. *Bulletin of Volcanology*, 73: 1353-1368.
- Jenkins, S.F., Magill, C.R. and McAneney, K.J., 2007. Multi-stage volcanic events: A statistical investigation. *Journal of Volcanology and Geothermal Research*, 161(4): 275-288.
- Jenkins, S.F., Wilson, T.M., Magill, C.R., Miller, V., Stewart, C., Blong, R., Marzocchi, W., Boulton, M., Bonadonna, C. and Costa, A., 2015. Volcanic ash fall hazard and risk. Chapter 3. In: S.C. Loughlin, R.S.J. Sparks, S.K. Brown, S.F. Jenkins and C. Vye-Brown (Editors), *Global Volcanic Hazards and Risk*. Cambridge University Press, Cambridge, UK, pp. 173. Open Access: cambridge.org/volcano.
- Komorowski, J.C., Legendre, Y., Caron, B. and Boudon, G., 2008. Reconstruction and analysis of sub-plinian tephra dispersal during the 1530 A.D. Soufrière (Guadeloupe) eruption: Implications for scenario definition and hazards assessment. *Journal of Volcanology and Geothermal Research*, 178(3): 491-515.
- Macgregor D (2015) History of the development of the East African Rift System: a series of interpreted maps through time. *J Afr Earth Sci* 101:232–252.
- Newhall, C. and Self, S., 1982. The Volcanic Explosivity Index (VEI) - An estimate of explosive magnitude for historical volcanism. *J Geophys Res Oceans Atmos*, 87(C2): 1231 - 1238.

- NGI (2009): Risk Assessment and Mitigation Measures for Natural and Conflict Related Hazards in Asia-Pacific. NGI Report 20071600-1.
- Pagani, M., Monelli, D., Weatherill, G., Danciu, L., Crowley, H., Silva, V., Henshaw, P., Butler, L., Nastasi, M., Panzeri, L., Simionato, M., Vigano, D., 2014. OpenQuake Engine: An Open Hazard (and Risk)
- Rickenmann, D. (2005): Runout Prediction Methods. In: Jakob, M., Hungr, O. (eds.) Debris-flow Hazards and Related Phenomena. Springer-Verlag Berlin Heidelberg. DOI: 10.1007/b138657
- Silva, V., Crowley, H., Pagani, M., Monelli, D., Pinho, R., 2013. Development of the OpenQuake engine, the Global Earthquake Model's open-source software for seismic risk assessment. Nat Hazards 72:1409–1427.
- Software for the Global Earthquake Model. Seismological Research Letters 85: 692–702. Poggi, V., Durrheim, R., Mavonga Tuluka, G., Weatherill, G., Gee, R., Pagani, M., Nyblade, A., Delvaux, D., 2017. Assessing Seismic Hazard of the East African Rift: a pilot study from GEM and AfricaArray. Bull. of Earth. Eng. 15:4499-4529.
- Tegeje, JA and Kervyn, M (2017): Review of Spatial and Temporal Distribution of Landslides in Tanzania. Journal of Ecosystem and Ecography, Volume 7, Issue 3. DOI: 10.4172/2157-7625.1000243
- UNISDR (2009): Global assessment report on disaster risk reduction. <https://www.unisdr.org/we/inform/publications/9413>
- Wells, D. L., and K. J. Coppersmith (1994). New empirical relationships among magnitude, rupture length, rupture width, rupture area and surface displacement, Bull. Seism. Soc. Am. 84:974-1002.

11 Appendix 1 scenario examples

11.1 LANDSLIDE EVENT DATA

Event Set

```

id - EastMoshiDebrisFlows01
geographic_area_bb - [37.33, -3.37, 37.48, -3.10]
geographic_area_name - Tanzania, Kilimanjaro, Kilimanjaro Region,
Moshi
creation_date - 2018-03-14
hazard_type - Landslide
time_start - None
time_end - None
time_duration - None
description - Debris flow zones on the southern slopes of Mountain
Kilimanjaro originating from steep ravines to the east and
northeast of the city of Moshi
bibliography - Rickenmann, D. (2005): Runout Prediction Methods.
In: Jakob, M., Hungr, O. (eds.) Debris-flow Hazards and Related
Phenomena. Springer-Verlag Berlin Heidelberg. DOI: 10.1007/b138657

```

Event

```

id - DebrisFlowRelease01
event_set_id - EastMoshiDebrisFlows01
calculation_method - simulated
frequency - None
triggering_hazard_type - Extreme Precipitation
description - Multiple simultaneous landslides triggered by
intense rainfall. Runouts are simulated using an empirical
relationship by Rickenmann (2005, Figure 13.1).

```

Footprint set

```

id - DebrisFlowFootprintSet01
event_id - DebrisFlowRelease01
process_type - Debris flow
imt - Binary index where 1 indicates landslide affected zone
data_uncertainty - Runout distances are based on empirical model
from different region, so affected zones are only a high-level

```

estimate. Deterministic simulation required for more precise mapping.

Footprint

```
id - FootprintW03.txt
footprint_set_id - DebrisFlowFootprintSet01

id - FootprintW04.txt
footprint_set_id - DebrisFlowFootprintSet01

id - FootprintW10.txt
footprint_set_id - DebrisFlowFootprintSet01
```

data - Tab-delimited text files with locations within the susceptible zones. Columns 1 and 2 indicate latitude and longitude in decimal degrees using GCS_WGS_1984 coordinate system. Datasets are based on rasterization of polygons at a 0.0005 degree resolution.

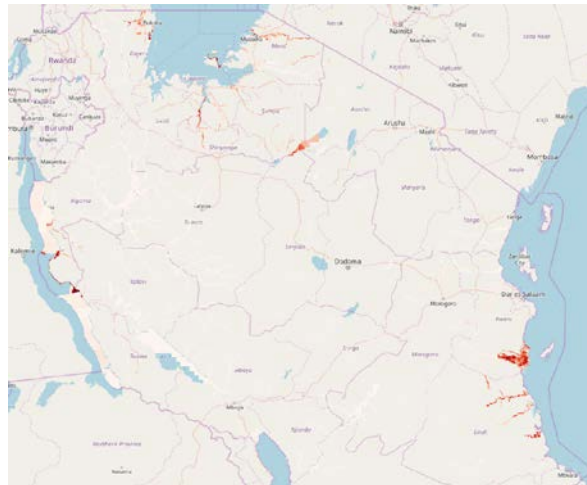
Vertices of the polygons sketched are included separately in the file Mudslide_footprints_vertices.txt

11.2 FLOOD EVENT DATA

Event Set

```
id - FL01
geographic_area_bb - [-10.28, 29.33, -2.00, 39.71]
geographic_area_name - UR Tanzania
creation_date - 2017-12-12
hazard_type - Flood
time_start - None
time_end - None
time_duration - None
description - Simulated maximum flood water depths for the entire country of UR Tanzania
bibliography -
https://www.preventionweb.net/english/hyogo/gar/2015/en/bgdocs/risk-section/CIMA%20Foundation,%20Improvement%20of%20the%20Global%20Flood%20Model%20for%20the%20GAR15.pdf
```

Event



```

id - TZ_01
event_set_id - FL01
calculation_method - simulated
occurrence_probability - None
occurrence_time_start - None
occurrence_time_end - None
occurrence_time_span - None
triggering_hazard_type - None
triggering_event_id - None
description - The event considered is one of the largest events
in the coastal zone of the UR Tanzania and is likely to
contribute to give a substantial contribution to the PML curve.

```

Footprint set

```

id - TZ_01_M1
event_id - FL01.TZ_01
process_type - Flood
imt - water depth
data_uncertainty - Equiprobable

```

Footprint

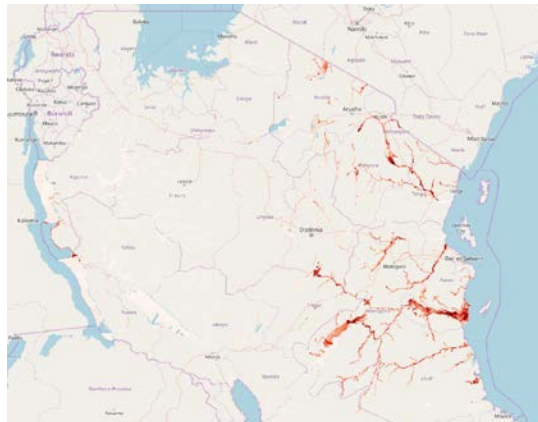
```

id - Scenario_TZ_01_M1
footprint_set_id - FL01.TZ_01.TZ_01_M1
data - a geotiff reporting the water depths values in m

data_uncertainty_2nd_moment - TZ_01_M2
triggering_footprint_id - None

```

Event



```

id - TZ_11
event_set_id - FL01
calculation_method - simulated
occurrence_probability - None
occurrence_time_start - None
occurrence_time_end - None
occurrence_time_span - None
triggering_hazard_type - None
triggering_event_id - None
description - The event considered is one of the largest events
Country wide in UR Tanzania and is likely to contribute to give
a substantial contribution to the PML curve.

```

Footprint set

```

id - TZ_11_M1
event_id - FL01.TZ_11
process_type - Flood
imt - water depth
data_uncertainty - Equiprobable

```

Footprint

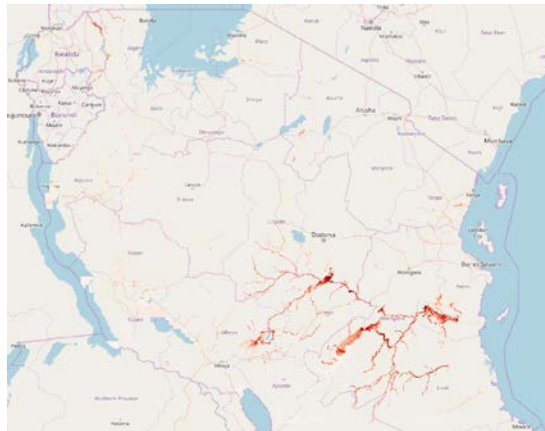
```

id - Scenario_TZ_11_M1
footprint_set_id - FL01.TZ_11.TZ_11_M1
data - a geotiff reporting the water depths values in m

data_uncertainty_2nd_moment - TZ_11_M2
triggering_footprint_id - None

```

Event



```

id - TZ_19
event_set_id - FL01
calculation_method - simulated
occurrence_probability - None
occurrence_time_start - None
occurrence_time_end - None
occurrence_time_span - None
triggering_hazard_type - None
triggering_event_id - None
description - The event considered is one of the largest events
in the southern UR Tanzania and is likely to contribute to give
a substantial contribution to the PML curve.

```

Footprint set

```

id - TZ_19_M1
event_id - FL01.TZ_19
process_type - Flood
imt - water depth
data_uncertainty - Equiprobable

```

Footprint

```

id - Scenario_TZ_19_M1
footprint_set_id - FL01.TZ_19.TZ_19_M1
data - a geotiff reporting the water depths values in m

data_uncertainty_2nd_moment - TZ_19_M2
triggering_footprint_id - None

```